Parasitology International 58 (2009) 36–44

Contents lists available at ScienceDirect

Parasitology International

journal homepage: www.elsevier.com/locate/parint

Proteome approach for identification of schistosomiasis japonica vaccine candidate antigen

Ekhlas Hamed Abdel-Hafeez [a], Mihoko Kikuchi [a,b], Kanji Watanabe [c], Takashi Ito [d,e], Chuanxin Yu [f], Honggen Chen [g], Takeshi Nara [h], Takeshi Arakawa [i], Yoshiki Aoki [c], Kenji Hirayama [a,e,*]

[a] Department of Immunogenetics, Institute of Tropical Medicine (NEKKEN), Nagasaki University, 1-12-4 Sakamoto, Nagasaki 852-8523, Japan
[b] Center for International Collaborative Research, Nagasaki University (CICORN), 1-12-4 Sakamoto, Nagasaki 852-8523, Japan
[c] Department of Parasitology, Institute of Tropical Medicine (NEKKEN), Nagasaki University, 1-12-4 Sakamoto, Nagasaki 852-8523, Japan
[d] Department of Biochemistry, Nagasaki University, School of Medicine 1-12-4 Sakamoto, Nagasaki 852-8523, Japan
[e] Global COE Program, Nagasaki University, 1-12-4 Sakamoto, Nagasaki 852-8523, Japan
[f] Jiangsu Institute of Parasitic Diseases, Meiyuan, Wuxi, Jiangsu 214064, PR China
[g] Jiangxi Provincial Institute of Parasitic Diseases, Nanchang 330046, PR China
[h] Department of Molecular and Cellular Parasitology, Department of Epidemiology and Environmental Health, Juntendo School of Medicine, Hongo 2-1-1, Bunkyo-ku,Tokyo 113-8421, Japan
[i] Division of Molecular Microbiology, Center of Molecular Biosciences, University of the Ryukyu, 1 Senbaru, Nishihara 903-0213, Okinawa, Japan

ARTICLE INFO

Article history:
Received 26 May 2008
Received in revised form 11 August 2008
Accepted 19 September 2008
Available online 7 October 2008

Keywords:
Schistosoma japonicum
Radiation-attenuated cercariae
Vaccine
Miniature pig
Proteome

ABSTRACT

Experimental vaccination with radiation-attenuated cercariae (RAC) confers possible practical levels of resistance to challenge infection by humoral and by cellular mechanism. Here, we aimed to identify possible vaccine antigens by using specific IgG antibody from RAC vaccinated miniature pig. Two milligrams of soluble egg antigen (SEA) or schistosomal worm antigen preparation (SWAP) was fractionated using two dimensional liquid chromatography (proteome PF 2D) consisted of high performance chromatofocusing (HPCF) and high resolution reversed phase chromatography (HPRP). Of the 42 HPCF fractions of SEA or SWAP, 26 (61.9%) or 15 (35.7%) showed positive dot blot reaction with RAC vaccinated serum respectively. The dot blot positive fractions were applied to the second HPRP column. One hundred and seven out of 26×96 of SEA fractions and 18 out of 15×96 SWAP fractions reacted with RAC vaccinated serum. From the positive fractions we chose 17 of SEA and 10 of SWAP that had no reactivity with normal cercariae infected (NCI) sera and had single peak of 214 nm; and automated N-terminal amino acid sequence based on in situ Edman Reaction was conducted. Four sequences were obtained and applied to the homology search in NCBI database. A total of eight candidate genes were listed up and their cDNA clones from schistosomula stage were obtained. Two of the recombinant proteins (AAW27472.1 and AXX25883.1) showed strong reactivity with the RAC vaccinated serum but marginal with NCI serum. This protocol using proteome PF 2D could be applicable in identifying immunoreactive proteins from crude extract for the development of vaccines or for diagnostics.

1. Introduction

Schistosomiasis is a parasitic disease which affects more than 200 million individuals in Africa, Asia and South America. It is endemic in 74 countries causing more than 250,000 deaths per year [1]. Despite two decades of comprehensive campaign for the control, the number of individuals with active schistosomiasis worldwide remains at about 200 million annually [2,3]. Vaccine has long been expected to be developed as a novel strategic tool for the control [4–6]. A comprehensive review on current status of vaccines for schistosomiasis had provided by McManus and Loukas [7].

There are three different approaches for isolation and identification of schistosome vaccine candidates [8,9]. Selection based on protective monoclonal antibodies such as glutathione-S-transferase (GST) [10] and triosephosphate isomerase (TPI) [11], by unique antigen recognition by strong natural resistance in humans [12] or animals [13], or by antigen selection using the radiation-attenuated cercariae vaccine (RAC) model [14–16]. For example, a fragment of myosin of *S. mansoni* (SmIrV-5); one of the vaccine candidate antigens selected by TDR/WHO committee [17], was identified using serum from mice exposed to RAC [18]. None of the antigens identified conferred equivalent efficacy of the vaccination using RAC [5,19,20]. There is a quantitative and/or qualitative difference between the immune responses generated by RAC vaccine and those by defined subunit vaccine [21,22]. Increased immunogenicity of

Abbreviation: RAC, radiated-attenuated cercariae; NCI, normal cercariae infected; NC, healthy control; SEA, soluble egg antigen; SWAP, schistosomal worm antigen preparation; HPCF, high performance chromatofocusing; HPRP, high resolution reversed phase chromatography.

* Corresponding author. Tel.: +81 95 819 7818; fax: +81 95 819 7821.
E-mail address: hiraken@nagasaki-u.ac.jp (K. Hirayama).

1383-5769/$ – see front matter © 2008 Elsevier Ireland Ltd. All rights reserved.
doi:10.1016/j.parint.2008.09.004

RAC is related to delayed and truncated pattern of migration, in contrast to the normal parasite [23]. In fact, radiation induces defects in the neuromuscular coordination of the developing larvae [24]. Accordingly, delayed parasite migration through skin or skin draining lymph nodes and lungs would mean that there is a greater opportunity for interaction of parasite antigen with the immune cells at these sites which may in turn favor the priming of the protective response.

The highest levels of resistance obtained in mice after vaccination with RAC require antibodies and T cells [25,26]. It is clear that protective immunity generated by RAC vaccines is mediated by acquired immune mechanisms that require the reactivation of antigen specific $CD4^+$ helper cells [27]. However, passive transfer experiments indicate that IgG antibodies are also the key mediators of this immunity [28–30].Thus, elucidation of antigens relevant to both humoral and cellular response may be critical for the development of an optimal vaccine.

Most of our knowledge on schistosomiasis is drawn from experiments in primates and rodents. Although primate model is relatively better but the high cost and ethical concerns make them difficult to be used [31]. Also the use of rodents has several problems as a model for schistosomiasis [32,33]. When we focus on RAC vaccine of *S. japonicum*, higher protection has been achieved in rhesus monkeys [34], in cattle [35,36] and in pigs [19]. Within the reservoir host animals, pig would be the easiest one compared with cattle or sheep, but still the major drawback of the domestic pig is the large body mass. For this reason we established a unique miniature pig model for human Schistosomiasis japonica [37]. In this study we aimed to identify the major antigenic molecules which are specifically recognized by RAC vaccinated serum of miniature pigs for identification of possible candidate schistosomiasis vaccine.

2. Materials and methods

2.1. Parasite

Chinese strain of *S. japonicum* was obtained from Jiangsu Provincial Institute of Parasitic Diseases Wuxi, Jiangsu Province, People's Republic of China. Cercariae were released from the infected snails by light induction as described [38]. Attenuation of the cercariae was carried out by 200 Gy of γ-irradiation at a rate of 33 Gy/min using ^{60}Co irradiator (Pony Industry CO. LTD. PS-3100sB, Osaka, Japan).

2.2. Preparation of cultured schistosomula

Cercariae were released from 100 infected snails in a beaker containing 200 ml of tap water under light for 2 to 3 h at room temperature and were passed through Sartorus Nylon spacer, mesh size 0.1 mm. The obtained suspension was centrifuged for 60 s at 1500 rpm (383 g) at 10 °C to concentrate cercariae. The cercariae were washed twice in Basal Medium Eagle (BME) (Gibco-Invitrogen Co., CA, USA) containing 15 mM of HEPES (Gibco-Invitrogen Co.), 300 units/l Penicillin (Gibco-Invitrogen Co.), 300 μg/l Streptomycin (Gibco-Invitrogen Co.) and 160 μg/l Gentamicin (Gibco-Invitrogen Co.) in aseptic condition. Transformation of cercariae to schistosomulae was carried out mechanically by shearing the tail using vortex for 3 min; and about 200–300 parasites/ml of the mechanically transformed shistosomulae were cultured in DMEM (Sigma-Aldrich Co., MO, USA) containing 1% Fetal calf serum (FCS) (Hyclone, UT, USA), 300 units/l penicillin and 300 μg/l streptomycin in 24 well plate (Corning, NY, USA) at 37 °C in 5% CO_2 incubator for 24 h. The cultured schistosomulae were collected by centrifugation, washed three times with phosphate buffered saline (PBS) and kept frozen at −80 °C until use [39].

2.3. Soluble worm antigen preparation (SWAP)

SWAP was obtained by the method described elsewhere [40]. Briefly, *S. japonicum* adult worms were obtained by perfusion of infected rabbits. After lyophilization, worms were homogenized in cold diethyl ether and centrifuged to remove lipids. The pellet was then freeze–thawed several times in PBS, pH 7.4 containing 1 mM phenyl methyl-sulphonyl fluoride (PMSF) and 2 μg/ml Leupeptin (Sigma). The homogenate was dialyzed against several changes of PBS at 4 °C, and centrifuged at 30,000 g for 50 min at 4 °C. The supernatant was filtrated through 0.22 μm filter (Millipore Co., MA, USA) and this was used as SWAP. Protein concentration was determined by BCA protein Assay Kit (Pierce Biotechnology, Inc., IL, USA).

2.4. Soluble egg antigen preparation (SEA)

Preparation of SEA was previously described [41]. Briefly, *S. japonicum* eggs were isolated from infected liver and intestine of rabbit. The purified eggs were finally adjusted to a concentration of 50,000 eggs/ml of PBS with 1 mM of PMSF, and 2 μg/ml Leupeptin (Sigma) and sonicated three times on ice for 10 min. The suspension was freeze–thawed several times and centrifuged at 30,000 g for 50 min at 4 °C. The supernatant was filtrated through 0.22 μm filter; and this was used as SEA. Protein concentration was determined by BCA protein assay.

2.5. Experimental animals, parasitological examinations and serum sample collection

Six-week-old male CLAWN strain miniature pigs (Japan farm, Kagoshima, Japan) weighing between 2.5 kg and 3 kg were used in this study. The pigs were fed with standard feed based on their body weights, with water ad libitum. Seven pigs were used, three for immunization with radiation-attenuated cercariae (RAC) of *S. japonicum*, three for infection with 200 cercariae (NCI) and one as a healthy control (NC). Sera were collected four weeks after vaccination and four weeks after challenge by drawing blood from auricular vein at indicated times. Before taking blood, pigs were anesthetized by intramuscular injection with 0.2 mg/kg midazolam (Yamanouchi Pharmaceutical Co., Ltd. Tokyo, Japan) and 40 μg/kg medetomidine (Orion Corp., Espoo, Finland). The first group of pigs was subjected to a single percutaneous exposure of 400 RAC using a cover slip as described [37]. Four weeks later, the first and second groups of pigs were challenged with 200 normal cercariae (NCI). The third group was used as a healthy control. Feces were collected every week and the number of eggs excreted into feces was counted as previously described [37]. Adult worms were recovered from the liver and mesenteric veins as described [20]. The experimental protocol was approved by the Animal Ethical Committee of Nagasaki University (No.0204250127-3).

2.6. SDS-PAGE and western blot analysis

SWAP and SEA were boiled for 5 min in reducing sample buffer containing 4% sodium dodecyl sulfate (SDS) and 50 mM Dithiothreitol (DTT), and electrophoresed by using 5–20% gradient SDS polyacrylamide gel (E-pagel®, Atto Co., Tokyo, Japan) [42]. For the western blot analysis, SEA and SWAP proteins separated by the E-pagel were transferred onto PVDF membrane (Millipore Co.). After blocking in 5% skimmed milk in Tris-buffer (TBS-Tween 20) (20 mM Tris–HCl, pH 7.5; 500 mM NaCl; 0.1% Tween 20) for 1 h at room temperature, the protein transferred-membrane was incubated with the 3000 times diluted test serum for 2 h at room temperature. After washing three times with TBS-Tween 20, the membrane was incubated in 10 ml of a secondary antibody solution containing 40,000 times diluted affinity Purified anti-porcine IgG antibody that is horseradish peroxidase

Table 1
Fecal egg excretion of RAC immunized and none immunized miniature pigs after challenge infection with 200 cercariae of *S. japonicum* Chinese strain

Examination time after challenge infection	EPG (egg per gram of feces)		P[c]
	RA[a] (n=3)	NC[b] (n=3)	
5th week	74.34±82.26	102.81±81.47	NS
(EPG of individual)	(190.65, 18.65, 13.71)	(45.03, 196.00, 67.4)	
6th week	265.03±151.25	413.42±171.92	0.028
(EPG of individual)	(438.78, 193.48, 162.82)]	(610.00, 291.13, 339.14)	
7th week	180.68±104.29	389.85±254.99	NS
(EPG of individual)	(298.61, 142.86, 100.57)	(681.03, 206.42, 282.10)	
8th week	156.24±99.28	558.26±181.23	0.026
(EPG of individual)	(265.91, 130.36,72.46)	(686.22, 637.68, 350.88)	
9th week	207.42±79.60	480.61±76.57	0.003
(EPG of individual)	(280.49, 219.18, 122.95)	(528.69, 520.83, 392.31)	

The values in parentheses represent the EPG for each pig.
[a] RA: vaccinated with 400 RAC.
[b] NC: no vaccination control.
[c] P values were calculated by two tailed Student's *t*-test.

(HRP) conjugated (Anti pig IgG (H+L)-HRP, AP166P, Chemicon International, CA, USA) and TBS-Tween 20 for 1 h at room temperature. After washing three times with TBS-Tween 20, reactive protein bands were visualized by exposing an x-ray film using ECL-Plus Western blotting Detection system (G. E. Healthcare, Amersham Biosciences, Buckinghamshire, UK).

2.7. Protein purification and fractionation

The protein purification and fractionation of SWAP and SEA were performed using Proteome Lab PF 2D system (Beckman Coulter, CA, USA) that is designed for two dimensional liquid chromatography consisted of a high-performance chromatofocusing (HPCF) in the first dimension followed by high-resolution reversed-phase chromatography (HPRP) in the second dimension. One milliliter of 2 mg/ml of either SWAP or SEA was introduced with a manual injector into the column for the first dimensional HPCF. The protein was bound to a strong anion exchanger followed by elution with a continuously decreasing pH (8.5–4.0) gradient (Beckman Coulter). The proteins were eluted based on their isoelectric point (pI), collected in a 96 deep-well plate (Beckman Coulter) [43]. The first dimensional fractions were directly applied to the second HPRP in a C18 column. The mobile phase consisted of two buffers, the first one 0.1% Trifluoroacetic acid (TFA) in water and the second one 0.08% TFA in acetonitrile. Separation was performed according to the Manufacturer's instruction protocol.

2.8. Dot blot ELISA

The fractions were blotted onto a PVDF membrane (Millipore Co.) using the Bio-Dot ® SF Micro filtration apparatus (Bio Rad Laboratories, Inc., CA, USA). Briefly, 20 µl of each fraction were blotted onto the PVDF membrane and the membrane was soaked in 5% skimmed milk in Tris-buffer (TBS-Tween 20) for 1 h at room temperature. The membrane was incubated with 1000 times diluted test serum for 2 h at room temperature. The reactivity of each dot with test serum was estimated by the dot blot ELISA using the same method described above in the western blotting. We selected positive dots when they showed increased intensity compared with those incubated with normal control serum. The criteria that used for selection of the positive/negative results of dot-ELISA are using two positive controls, the crude antigens of SWAP and SEA, and PBS as a negative control. All the positive fractions of the first dimension were sequentially applied to the second dimensional HPRP.

Table 2
Worm numbers recovered from each group of miniature pigs

Pig group	Worm burden			
	Total	Male	Female	Reduction rate[b]
RA 1	5	4	1	96.4%
RA 2	42	36	6	69.7%
RA 3	51	44	7	63.2%
Average	32.67	28.0	4.67	76.4%
NC 1	160	135	25	–
NC 2	117	87	30	–
NC 3[a]	–	–	–	–
Average	138.5	111.0	27.5	–

NC3[a]: this pig died at the 9th week after infection due to sudden death.
Reduction rate [b]: The worm reduction rate=(the average worm burden in the control group−the worm burden in the vaccinated group)/(the average worm burden in the control group)×100.

2.9. Amino acid sequencing

Fractions from the second dimensional HPRP were analyzed by dot blot ELISA and positive fraction was subjected to amino acid sequencing. Two hundred microliters of positive fraction was spotted onto Polybrene-coated glass fiber discs. Subsequently proteins were sequenced with an automated protein sequencer (ABI Model cLc; Applied Biosystem, CA, USA).

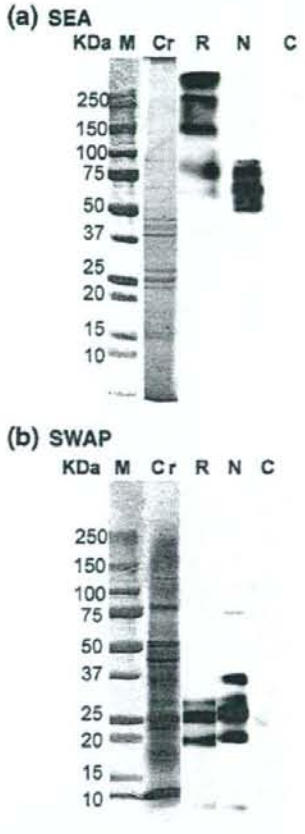

Fig. 1. SDS-PAGE and western blot analysis of RAC (R), NCI (N) and NC (C) sera of miniature pig for the specific IgG against (a) SEA and (b) SWAP. Lane M: molecular weight marker; lane Cr: CBB staining of the crude extract; lanes R, N and C: Western blot pattern probed with a panel of sera; lane R: RAC serum; lane: N. NCI serum and lane: C NC serum. Sera were diluted 3000 times.

2.10. Homology search

The obtained amino-terminal sequences were blast-searched for their homology with the genes deposited in the *S. japonicum* database in NCBI using BLAST/blastp suite programs, in non redundant Gene Bank Coding Sequence (CDS). After homologous genes were listed up, further selection was performed according to the following criteria; the homologous area should be located at the N-terminus sequences and its deduced pH must be within the pI range of first dimensional fraction.

2.11. mRNA analysis

To confirm mRNA expression of the candidate genes in the different stages of the parasites, total RNA was extracted from cercariae, 24 h cultured schistosomulae, eggs, and adult worms of *S. japonicum* according to the instruction manual of Micro-to-midi total RNA purification system kit (Invitrogen Co.). The first strand cDNA was synthesized from the total RNA by using oligo (dT) primer according to the instruction manual of high capacity cDNA reverse transcription Kit (Applied Bio systems) and was used as template for reverse transcript PCR using a set of primers that were designed from the candidate gene as indicated in the Table 4. *S. japonicum* actin gene primers were used as an internal reference. RT-PCR was performed by the following condition of 42 cycles of 30 s at 94 °C, 50 s at 55 °C and 2 min at 72 °C for all samples. PCR products were subsequently separated on 1% agarose gel, stained with ethidium bromide and visualized under UV light. The resulting PCR products were cloned into pCR 2.1 using TOPO-TA cloning Kit (Invitrogen Co.), sequenced using Big-Dye V.1.1 terminator cycle sequencing Kit (Applied Biosystem) and analyzed on an ABI 3710 DNA Sequencer (Applied Biosystem) for confirmation with database sequences.

2.12. Production of recombinant protein

Reverse-PCR products from cercarial mRNA purified from agarose gel were cloned into the pET/100 D-TOPO expression vector (Invitrogen Co.) and transformed into chemically competent TOP10 *Escherichia coli* (Invitrogen Co.) according to the manufacturer's protocol. Cells were plated onto LB-Ampicillin (50 μg/ml) plates and incubated for 18 h at 37 °C. Ten positive clones were identified and were grown for 18 h in 6 ml LB medium containing Ampicillin (50 μg/ml) and plasmids prepared using a Gene Elut™ plasmid Miniprep kit (Sigma). Plasmids were then digested with Nhe I and Sac I (New England Biolabs, MA,USA) for 2 h at 37 °C and the inserts detected by separating the DNA on a 1% agarose gel stained with ethidium bromide and visualized under U.V. light.

To confirm the correct orientation and in frame, the inserts were sequenced using Big-Dye V.1.1 terminator cycle sequencing Kit (Applied Biosystem) and analyzed on an ABI 3710 DNA Sequencer (Applied Biosystem). Plasmid DNA containing expression constructs was transformed into BL21 Star™ (DE3) One Shot® *E. coli* (Invitrogen Co.) for recombinant protein expression. Briefly, 10 ng of plasmid DNA was transformed into the bacteria by heat shocking at 42 °C for 30 s. Transformed bacteria were grown overnight at 37 °C in LB medium supplemented with either 100 μg/ml ampicillin or 50 μg/ml

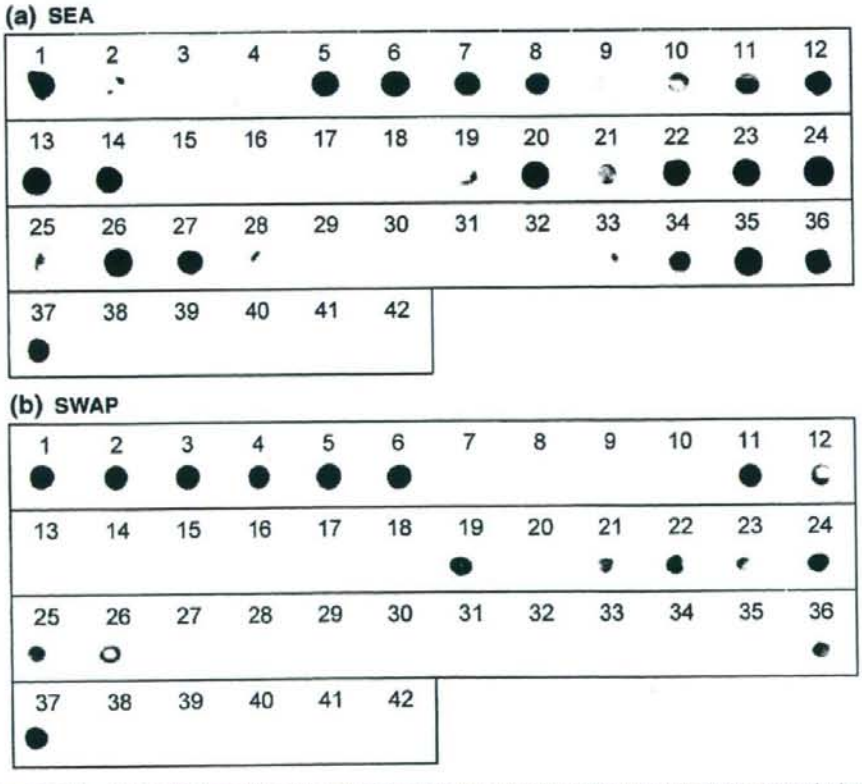

Fig. 2. Dot blot analysis of (a) SEA and (b) SWAP fractions of HPCF using pooled RAC vaccinated sera were diluted 1000 times. Dot blot has been repeated twice and the representable positive fractions to RAC serum were selected.

Table 3
Dot blot analysis of the first and second fractions of SEA and SWAP that reacted with RAC vaccinated and/or NCI serum from miniature pigs

Sequential screening steps		No. of the RAC positive fractions (%)	
		SEA (%)	SWAP (%)
1st dimension	(42 Frs. of SEA, 42 Frs. of SWA)	26 (61.9)	15 (35.7)
2nd dimension	(2496 Frs. of SEA, 1440 Frs. of SWA)	107 (4.3)	18 (1.3)
NCI (−)	(107 Frs. of SEA, 18 Frs. of SWA)	61 (57)	10 (55)
Single peak (+)	(61 Frs. of SEA, 10 Frs. of SWA)	17 (27.87)	10 (100)

Frs.: Fractions.
NCI (−): Dot blot fractions that did not react with Normal Cercaria Infection serum.
Single peak (+): Dot blot fractions that have single retention peak were selected to amino acid sequencing.

carbenicillin prior to pilot expression by the addition of Isopropyl β-D-1-thiogalactopyranoside (IPTG) as an inducer according to the manufacturer's protocol (Invitrogen Co.). Briefly, 10 ml of LB medium containing 100 μg/ml ampicillin or 50 μg/ml carbenicillin was inoculated with 500 μl of an overnight culture and allowed to grow for 2 h at 37 °C with shaking until they reached mid-log phase of growth. IPTG was then added to a final concentration of 0.1 mM to 0.5 mM and a 500 μl aliquot was removed from the culture, centrifuged at 10,000 g in a micro centrifuge for 30 s. The supernatants were removed and the cell pellets frozen at −20 °C. Remaining cultures were incubated at 37 °C with shaking and 500 μl aliquots were removed after 1, 2, 4 and 6 h post-induction. Individual sample was analyzed by SDS-PAGE and western blot for detection of recombinant protein using Anti-His G-HRP Antibody (Invitrogen Co.).

3. Results

3.1. Protective response in miniature pig vaccinated with radiation-attenuated cercariae (RAC)

The mean of fecal egg excretion of RAC vaccinated group was significantly reduced at 6th, 8th and 9th weeks post infection, when compared to the control group as shown in Table 1. The recovered worm number after the perfusion also indicated the vaccination effect of RAC as shown in Table 2.

3.2. Antigen recognition by sera from the vaccinated miniature pigs

We aimed to identify the antigenic molecules reactive with RAC vaccinated serum of miniature pigs but not with serum from those just infected with 200 cercariae for 4 weeks. As a target antigen preparation, we used SEA and SWAP antigens [16].

Pooled sera obtained 4 weeks after the RAC vaccination recognized antigenic molecules of 263, 255, 155, 130, 78, 55 and 20 kDa from SEA as shown in lane (R) of Fig. 1a. Whereas sera obtained 4 weeks post challenge with 200 normal cercariae, recognized antigens of 253, 155, 130, 74, 60, and 37.5 kDa (lane N of Fig. 1a). When we used SWAP, pooled sera obtained 4 weeks after the RAC vaccination recognized antigens of 70, 27, 21 and 10 kDa as shown in lane R of Fig. 1b. Sera obtained 4 weeks post challenge with normal cercariae recognized antigens of 150, 71, 36, 27, 21 and 10 kDa (lane N, Fig. 1b). The pooled sera used in this experiment were diluted 3000 times.

3.3. First dimension: high-performance chromatofocusing (HPCF)

Following the HPCF fractionation of SEA and SWAP 42 fractions were obtained. All the 42 fractions from SEA or SWAP were tested for reactivity with RAC vaccinated pooled serum as shown in Fig. 2a and b. Totally 26 SEA and 15 SWAP fractions were reacted to RAC vaccinated pooled serum as shown in Table 3.

3.4. Second-dimension: high performance reversed-phase chromatography (HPRC)

Those 26 and 15 dot blot positive fractions of SEA and SWAP respectively, from the first dimension (HPCF) were subjected to further fractionation by the HPRC. The Proteome maps of the second dimensional separation are shown in Fig. 3a and b.

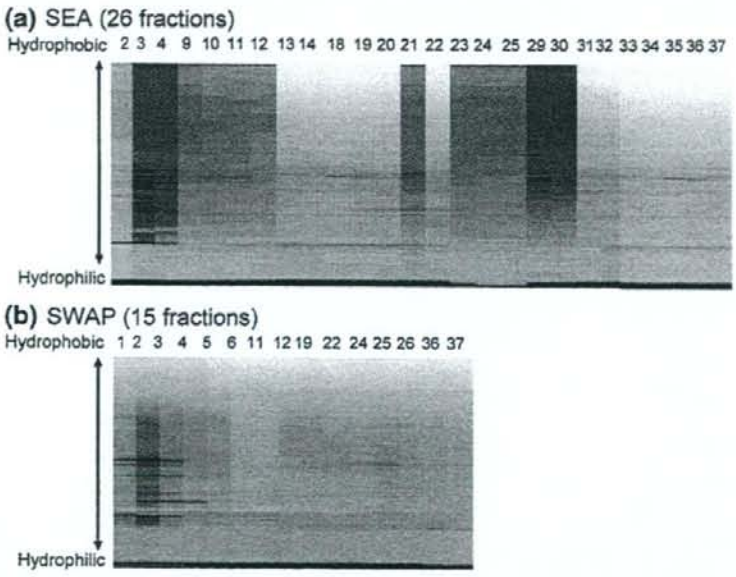

Fig. 3. The Proteo Vue ® MAP of the second dimensional separation for the positive dot blot fractions from SEA (a) and SWAP (b). Hydrophobicity of each fraction is expressed by its retention time. Each band represents Optical Density of a peptide at 214 nm. The fraction numbers of the first column are shown on top of the figures.

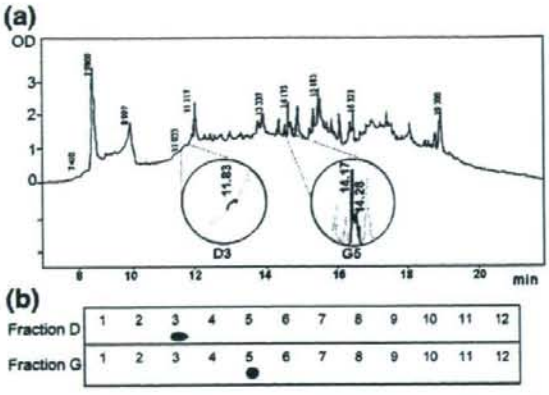

Fig. 4. Representative of the second column separation of the first fractions (fraction No.2 of SEA) (a) and the dot blots analysis for the fraction No. 2 of SEA (b). (a) The optical densitometry pattern (OD at 214 nm) is represented. The x axis represents retention time in min according to the concentration of acetonitrile in the mobile phase. (b) D3 and G5 are the two fractions obtained from the 96-well plate that was used for collection of the second column separation.

Elution pattern of the fraction number 2 of SEA after the second column is shown in Fig. 4a, as an example. All the fractions obtained after the second column were tested for reactivity against the RAC vaccinated serum. Out of the 2496 SEA and 1440 SWAP fractions, 107 and 18 fractions reacted with the RAC vaccinated serum respectively, as shown in Table 3. These 107 and 18 positive fractions were further tested for reactivity with normal cercariae infected (NCI) serum. Out of the 107 SEA and18 SWAP fractions, 46 and 8 fractions reacted with NCI serum respectively (Table 3). Dot blot pattern for fraction number 2 of SEA after second column separation was shown in Fig. 4b as an example. D3 and G5 fractions showed strong reactivity and D3 fraction had single retention peak while G5 fraction had two peaks as shown in Fig. 4a. The pooled sera used in dot blotting experiments were diluted 1000 times.

3.5. Amino acid sequencing

As shown in Table 3, after identification of 107 SEA and 18 SWAP fractions, we selected 61 SEA and 10 SWAP fractions by excluding the fractions reactive to NCI serum. For amino acid sequencing, we analyzed their retention peak patterns as shown in Fig. 4a, and picked 17 from SEA and 10 from SWAP that had single peak. Finally we obtained four N-terminal sequences, 2 from SEA and 2 from SWAP as shown in Table 4.

3.6. Homology search

The four identified N-terminal amino acid sequences were applied to the NCBI/BLAST/blastp suite programs. After the homology search we set the selection criteria of the candidate genes as follows, (1) high homology on the N-terminal sequences (2) deduced pH compatible with the pI range of first dimension. Two candidate genes for each amino acid sequence were selected as shown in Table 4.

Table 4
The amino acid sequences obtained from the fractions and the candidate genes with their homology and pI range

Fraction no.	pH range	N-terminal seq.	Identified homology	Accession no.	pI[a]
F29.2E. SEA	pH<4.80	MCVLPVD	60 CILPVD 65	AAX24607.2	4.70
			39 CVLP–43	AAW27155	4.60
F2.3D.SEA	8.49–8.4	MAVLPPIYKYL	3——PILYKYL 9	AAW27472.1	8.03
			281 MAVLP——— 285	AAW26143.1	8.02
F12.H1. SWAP	8.40–8.10	VPTNQN	415-PTNQ-418	AAW27566	8.39
			211-PTSQN 215	AAW26607.1	8.40
F12.F1. SWAP	8.40–8.10	KRRGPPGEER	131-RRSNPPTEE-139	AAW27690.1	8.49
			19——PPSEE–23	AAX25883.1	8.49

[a] pI: has been calculated from DNAstar software (DNASTAR Inc., Madison, WI, USA).

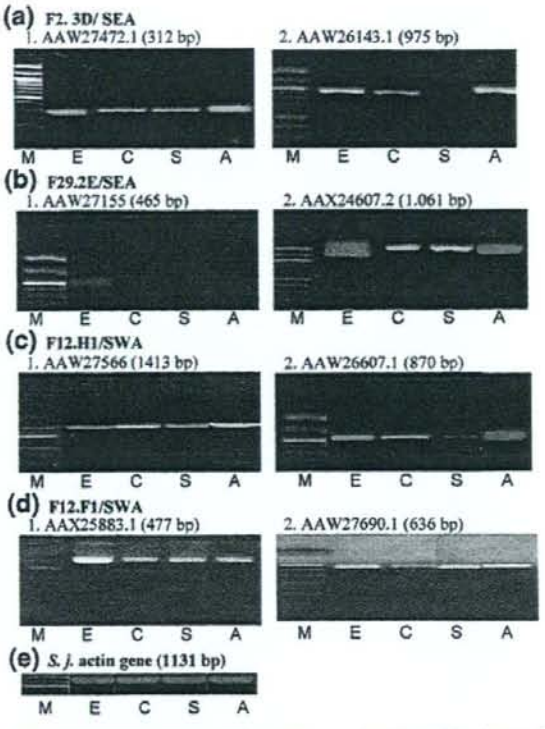

Fig. 5. mRNA expression of the selected candidate genes from different developmental stages of *S. japonicum*. PCR fragments with expected size amplified from the different stages of the *S. japonicum* were obtained using primer sets designed for the eight candidate genes and the actin gene as a control. Lane M: molecular weight maker; lane E: egg; lane C: cercariae; lane S: 24 h cultured schistosomula; lane A: adult worm. (e) *Schistosoma japonicum* actin gene.

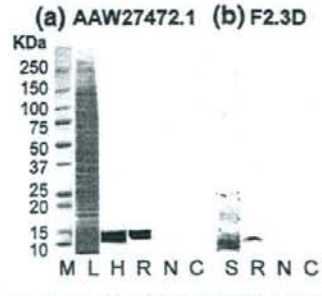

Fig. 6. Reactivity of the recombinant protein of AAW27472.1 (a) and its original fraction, F2.3D/SEA (b) with RAC vaccinated serum. (a) Lane M: molecular weight marker; lane L: CBB stained pattern of total lysate after induction with IPTG. Lanes H, R, N and C Western blotting patterns of the total lysate probed with a panel of sera; lane H: Anti histidine tag antibody; lane R: RAC serum; lane N: NCI serum; lane C: NC serum. (b) Lane S: Silver staining patterns of the original fraction, F2. 3D fraction. Lanes R, N and C: Western blotting patterns of the F2. 3D fraction probed with a panel of sera; lane R: RAC serum; lane N: NCI serum and lane C: NC serum.

3.7. Expression of mRNA encoding the candidate genes in different developmental stages

mRNA from eggs, cercariae, 24 h culture schistosomulae and adult worms of the Chinese strain of *S. japonicum* was used for RT-PCR amplification of the selected candidate genes. All the candidate genes were expressed in all the stages of the parasite, as shown in Fig. 5, except for the genes AAW27155 that was expressed only in the egg stage and AAW26143.1 that is expressed in the egg, cercariae and adult but not in schistosomulae (Fig. 5). All the amplified PCR fragments had exactly the expected molecular weight as in the NCBI database.

3.8. Recombinant and native protein reactivity with RAC vaccinated serum

Protein expression in *E coli* using recombinant pET100/D-TOPO expression vector bearing each PCR fragment was confirmed by the detection of a band in Coomassie Brilliant blue stained SDS-PAGE after IPTG induction and by western blotting probed with Anti His-tag Antibody or with vaccinated sera (data not shown). Two candidate genes named AAW27472.1 (Fig. 6) and AAX25883.1 (Fig. 7) with recombinant proteins having molecular weights 15.5 kDa and 24 kDa respectively were strongly recognized by RAC vaccinated sera but not reactive with NCI or NC sera. While the recombinant protein AAW27690.1 whose molecular weight was 35 kDa showed weak reactivity with RAC vaccinated serum but strong reactivity with NCI as shown in Fig. 7. Original native protein fractions of AAW27472.1, AAX25883.1 and AAW27690.1 that were F2.3D for AAW27472.1 and F12.1F for the latter two genes were analyzed by the western blotting analysis to compare with the recombinant protein patterns. As is shown in Fig. 6, native protein that corresponds to the same molecular weight around 11 kDa of the recombinant was detected by RAC serum.

Fig. 7 also shows strong reactive band of around 18 kDa in the F12.1F native fraction with RAC serum but not with NCI serum that may correspond to the AAX25883.1 recombinant protein of 21 kDa. Interestingly F12.1F fraction contained reactive band of 25 kDa with NCI serum that almost correspond to AAW27690.1 recombinant pattern.

4. Discussion

We have already reported that high levels of protective immunity were obtained by UV-attenuated cercaria vaccination in Chinese domestic pigs [20]. In this study we used CLAWN miniature pigs for vaccination with RAC and observed a comparable level of protective immunity as seen in the domestic pigs (Table1). Previous studies have shown that serum of RAC vaccinated mice can transfer protective immunity to naive recipients [25,44]. We concentrated on the analysis of antibodies in the development of resistance in this RAC vaccine miniature pig model.

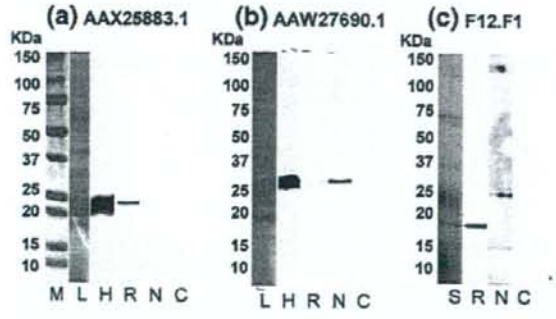

Fig. 7. Reactivity with RAC vaccinated serum of the recombinant proteins of AAX25883.1 (a) and AAW27690.1 (b) and that original fraction, F12.1F SWAP (c). (a) and (b) Lane M: molecular weight marker; lanes L: CBB stained pattern of total lysate after induction with IPTG. Lanes H, R, N and C: Western blot patterns of the total lysate probed with a panel of sera; lanes H: Anti histidine tag antibody lanes R: RAC serum; lanes N: NCI serum and Lanes C: NC serum. (c) Lane S: Silver staining patterns of the original fraction F12. F1 fraction). Lanes R, N and C: Western blotting patterns of the F12. F1 fraction probed with a panel of sera; lane R: RAC serum; lane N: NCI serum and lane C: NC serum.

In the present study, sera from RAC vaccinated pigs reacted with a number of proteins of SEA whereas sera collected from NCI showed different pattern of reaction (Fig. 1a).

The strong reactivity to SEA by the RAC vaccinated and NCI pigs could be explained by cross-reactivity of the provoked antibodies against components of cercaria to schistosomula stage worms or by the existence of common molecules shared between young worm and eggs. The significant difference of the reactive SEA proteins against RAC vaccinated and NCI sera suggests that the mode of immunization is different between those two methods [45,46].

It is well known that much of the antibodies of infected subjects are directed against carbohydrate determinants from the adult worms and the eggs [47]. We confirmed our major RAC vaccinated antibodies were directed against peptide by treating crude SEA and SWAP with glycopeptidase A, to remove the glycoconjugates. This treatment did not abolish the basic reactivity detected by the western blotting patterns of SEA or SWAP (data not shown).

Then we tried to identify a series of unique proteins that are recognized by RAC vaccinated sera but not by normal cercaria infected sera (NCI). As shown in Fig. 2 and Table 3, two-dimensional (2D) liquid chromatography successfully resolved the peptides that were shown to be reactive to RAC vaccinated serum. Although it is not clear that the 2D-LC has significant advantage over the 2D-SDS PAGE, using 2nd dimensional column, we could physically separate totally 2496 SEA fractions from 42 positive fractions of the first dimensional column and identified 107 fractions that were specifically reactive with RAC serum. Separation of intact proteins coupled with fraction collection was another advantage for this method [43]. Although our Edman degradation method could not identify many peptides, the discrimination ability from such a crude extract can be tolerated for further study.

We successfully obtained enough length of N-terminal sequences; 4 fractions out of 27 (Table 4). As shown in Figs. 6 and 7, even after the 2D column separation, each fraction contained several proteins as visualized by silver staining or by western blotting. The overall efficiency of the N-terminal sequencing of the fractions by the Edman Reaction is dependant on the purity and quantity so that we might have picked up major peptide's sequences in terms of quantity. Of course there is a fact that many schistosomal proteins were glycosylated and were possibly N-terminally blocked for the Edman Reaction. There is no doubt that MS-based protein identification is much faster and technically easier and currently the first choice over Edman degradation. Despite the fact that most of biological samples are a mixture even after physical separation as used in this study, the power of MS-based protein identification currently available should enable estimation of likeliness and relative abundance of identified proteins based on the number of peptides and coverage. The MS-based method must be more promising for this kind of identification.

After we got four sequences, the current database of ESTs from *S. japonicum* was used for the homology search. Unexpectedly, we have got only a limited level of homology to all the input sequences as was also noticed in the previous study [48]. Because of a large size of *S. japonicum* genome, it has not been subjected to full scale genome sequencing; [49,50]. Of course ESTs do not cover full length of the coding regions and a limited portion of transcripts are likely deposited in the EST database [51]. In order to increase the probability of selection of the candidate genes that were picked by their homology, pI was set as a second criterion for the selection (Table 4). His-tag fused recombinant proteins from the entire listed candidate genes were confirmed by western blotting using anti-his tag antibody and by

their expected molecular weights, and only three recombinant proteins of AAW27472.1, AAX25883.1 and AAW27690.1 showed reactivity to RAC vaccinated serum.

The recombinant proteins obtained from the cloned AAW 27472.1 and AX25883.1 were highly reactive to RAC vaccinated serum but marginal with NCI serum that exactly reproduced the original fraction's behavior (Figs. 6 and 7). While the recombinant protein obtained from the cloned AAW27690.1 showed weak reactivity with RAC vaccinated serum, it showed strong reactivity with NCI as shown in Fig. 7. Therefore, AX25883.1 is more probable to match with the obtained N-terminal sequence.

The expected molecular weight of AAW27472.1 was 12.475 kDa but the protein in original purified fraction showed about 11 kDa as shown in Fig. 6. This may be a result of post-translation modification that often occurs in schistosomes [52]. AAW27472.1 was revealed to be a hypothetical protein, but had 23% homology with Cathepsin B endopeptidase (*S. japonicum*), and had 26% homology with cathepsin B endopeptidase (*S. mansoni*). In contrast to AAW27472.1, the expected molecular weight of AAX25883.1 was 18 kDa, and the protein in original purified fraction showed same molecular weight as shown in Fig. 7. AAX25883.1 was revealed to be a Syntaxin N-terminus domain that is a neuron system-specific protein implicated in the docking of synaptic vesicles with the presynaptic plasma membrane and had 23% homology with crystal structure of the 26 kDa glutathione *S*-transeferase of *S. japonicum*. The expected molecular weight of AAW27690.1 was 25 kDa, and the protein in original purified fraction, showed the same molecular weight as expected as shown in Fig. 7. AAW27690.1 was revealed to be a NADH ubiquinone oxidoreductase subunit of NDUFA12 and had 26% homology with "NADH dehydrogenase subunit 5". As the original purified fraction showed a reactive band around 25 kDa, this may be explained by the same reason as AAW27472.1.

In the present study, we have focused on the identification of soluble proteins and did not analyse the membrane protein that is expected to be another source of vaccine candidates. This 2D column system is applicable to the detergent solubilized membrane proteins using 2% Trion X-100 [53]. Membrane protein must be the next target for our study.

Although we have not yet examined the efficacies of these subunit candidate vaccines, we concluded that our 2D column protein fractionation system was simple and effective to identify the immuno-reactive proteins from crude extract.

Acknowledgements

This study was supported in part by the Grant-in-Aid for 21c COE program, Nagasaki University (2005–2010) and Grant-in-Aid for Exploratory Research (19659106) from the Ministry of Education, Culture, Sports, Science and Technology (MEXT), Health and Labour Sciences Research Grants (Research on Emerging and Re-emerging Infectious Diseases, H18-Shinko-Ippan-008) and Health and Labour Sciences Research Grants (Research on International Cooperation for caring Societies, H19-Kokui-Shitei-004) from the Ministry of Health, Labour and Welfare of Japan. And grant from US-Japan-Cooperative Medical Science Program (Parasitic Disease). E. H. A. is a recipient of the Egyptian government scholarship.

References

[1] Van der Werf MJ, De Vlas SJ, Brooker S, Looman CW, Nagelkerke NJ, Habbema JD, et al. Quantification of clinical morbidity associated with schistosome infection in sub-Saharan Africa. Acta Trop 2003;86:125–39.
[2] Bergquist NR. Schistosomiasis vaccine development: progress and prospects. Mem Inst Oswaldo Cruz 1998;93:95–101.
[3] Ross AG, Bartley PB, Sleigh AC, Olds GR, Li Y, Williams GM, et al. Schistsomaiasis. N Engl J Med 2002;346:1212–20.
[4] McManus DP. The search for a vaccine against schistosomiasis – a difficult path but an achievable goal. Immuno-Rev 1999;171:149–61.
[5] McManus DP, Bartley PB. A vaccine against Asian schistosomiasis. Parasitol Int 2004;53:163–73.
[6] Bergquist NR, Leonardo LR, Mitchell GF. Vaccine-linked chemotherapy: can schistosomiasis control benefit from an integrated approach? Trends Parasitol 2005;21:112–7.
[7] McManus DP, Loukas A. Current status of vaccines for schistosomiasis. Clin Microbiol Rev 2008;21:225–42.
[8] McManus DP. Prospects for development of a transmission blocking vaccine against *Schistosoma japonicum*. Parasite Immunol 2005;27:297–308.
[9] Wu ZD, Lü ZY, Yu XB. Development of a vaccine against *Schistosoma japonicum* in China: a review. Acta Trop 2005;96:106–16.
[10] Xu CB, Verwaerde C, Grzych J-M, Fontaine J, Capron A. A monoclonal antibody blocking the *Schistosoma mansoni* 28-kDa glutathione S transferase activity reduces female worm fecundity and egg viability. Eur J Immunol 1991;21:1801–7.
[11] Harn DA, Gu W, Oligino LD, Mitsuyama M, Gebremichael A, Richter DA. Protective monoclonal antibody specifically recognizes and alters the catalytic activity of schistosome triose-phosphate isomerase. J Immunol 1992;148:562–7.
[12] Acosta LP, Aligui GD, Tiu WU, McManus DP, Olveda RM. Immune correlate study on human *Schistosoma japonicum* in a well-defined population in Leyte, Philippines: I. Assessment of resistance versus susceptibility to *S. japonicum* infection. Acta Trop 2002;84:127–36.
[13] Techau ME, Johansen MV, Lind P, Ornbjerg N. The effect of colostrum on pigs prenatally or postnatally exposed to *Schistosoma japonicum*. Parasitology 2004;129:597–604.
[14] Hooker CW, Brindley PJ. Cloning of a cDNA encoding SjlrV1, a *Schistosoma japonicum* calcium-binding protein similar to calnexin, and expression of the recombinant protein in *Escherichia coli*. Biochim Biophys Acta 1999;1429:331–41.
[15] Zhang Y, Taylor MG, McCrossan MV, Bickle QD. Molecular cloning and characterization of a novel *Schistosoma japonicum* irradiated vaccine-specific antigen, Sj14-3-3. Mol Biochem Parasitol 1999;103:25–34.
[16] Richter D, Harn DA. Candidate vaccine antigens identified by antibodies from mice vaccinated with 15- or 50-kilorad-irradiated cercariae of *Schistsoma mansoni*. Infect Immun 1993;61:146–54.
[17] Bergquist NR, Colley DG. Schistosomiasis vaccines: research to development. Parasitol Today 1998;14:99–104.
[18] Dalton JP, Tom DT, Strand M. Cloning of a cDNA encoding a surface antigen of *Schistosoma mansoni* schistosomula recognized by sera of vaccinated mice. Proc Natl Acad Sci 1987;84:4268–72.
[19] Shi YE, Jiang CF, Han JJ, Li YL, Ruppel A. Immunization of pigs against infection with *Schistosoma japonicum* using ultraviolet-attenuated cercariae. Parasitology 1993;106:459–62.
[20] Chen H, Nara T, Zeng X, Masao Wu SG, Fangyu WJ, Kojima YS, et al. Vaccination of domestic pig with recombinant paramyosin against *Schistosoma japonicum* in China. Vaccine 2000;20:2142–6.
[21] Pearce EJ, James SL, Hieny S, Lanar DE, Sher A. Induction of protective immunity against *Schistosoma mansoni* by vaccination with schistosome paramyosin (Sm97), a nonsurface parasite antigen. Proc Natl Acad Sci 1988;85:5678–82.
[22] Tarrab-Hazdai RF, Brenner LSV, Horowitz S, Eshhar Z, Arnon R. Protective monoclonal antibody against *Schistosoma mansoni*: antigen isolation, characterization, and suitability for active immunization. J Immunol 1985;135:2772–9.
[23] Mastin AJ, Bickle QD, Wilson RA. *Schistsoma mansoni*: migration and attrition of irradiated and challenge schistosomula in the mouse. Parasitology 1983;87:87–102.
[24] Harrop R, Wilson RA. Irradiation of *Schistsoma mansoni* cercariae impairs neuromuscular function in developing schistosomula. J Parasitol 1993;79:286–9.
[25] Jwo J, LoVerde PT. The ability of fractionated sera from animals vaccinated with irradiated cercariae of *Schistosoma mansoni* to transfer immunity to mice. J Parasitol 1989;75:252–60.
[26] Coulson PS, Wilson RA. Recruitment of lymphocytes to the lung through vaccination enhances the immunity of mice exposed to irradiated schistosomes. Infect Immun 1997;65:42–8.
[27] Hewitson JP, Hamblin PA, Mountford AP. Immunity induced by the radiation-attenuated schistosome vaccine. Parasite Immunol 2005;27:271–80.
[28] Moloney NA, Webbe G. Antibody is responsible for the passive transfer of immunity to mice from rabbits, rats or mice vaccinated with attenuated *Schistsoma japonicum* cercariae. Parasitology 1990;100:235–9.
[29] Soisson LA, Reid GD, Farah IO, Nyindo M, Strand M. Protective immunity in baboons vaccinated with a recombinant antigen or radiation-attenuated cercariae of *Schistosoma mansoni* is antibody-dependent. J Immunol 1993;151:4782–9.
[30] Kariuki TM, Farah IO, Yole DS, Mwenda JM, Van Dam GJ, Deelder AM, et al. Parameters of the attenuated schistosome vaccine evaluated in the olive baboon. Infect Immun 2004;72:5526–9.
[31] Von Lichtenberg F, Sadun EH, Cheever AW, Erickson DG, Johnson AJ, Boyce HW. Experimental infection with *Schistosoma japonicum* in chimpanzees. Am J Trop Med Hyg 1971;206:850–93.
[32] Moloney NA, Hinchcliffe P, Webbe G. Cross protection between a laboratory passaged Chinese strain of *Schistosoma japonicum* and field isolates of *S. japonicum* from China. Trans R Soc Trop Med Hyg 1989;83:83–5.
[33] Hope M, Duke M, McManus DP. A biological and immunological comparison of Chinese and Philippine *Schistosoma japonicum*. Int J Parasitol 1996;26:325–32.
[34] Hsu SYL, Hsu HF, Osborne JW. Immunization of rhesus monkeys against schistosome infection by cercariae exposed to high doses of X-radiation. Proc Soc Exp Biol Med 1969;131:1146–9.
[35] Li Hsü SY, Hsü HF, Shou Tai Xu, Hui Shi Fu, Yi Xun He, Clarke WR, et al. Vaccination against bovine schistosomiasis japonica with highly X-irradiated schistosomula. Am J Trop Med Hyg 1983;32:367–70.

[36] Hsu SYL, Xu ST, He YX, Shi FH, Shen W, Hsü HF, et al. Vaccination of bovines against schistosomiasis japonica with highly irradiated schistosomula in China. Am J Trop Med Hyg 1984;33:891–8.
[37] Watanabe K, Kikuchi M, Ohno A, Mohamed RT, Nara T, Ubaleeb R, et al. The miniature pig: a unique experimental model for *Schistosoma japonicum* infection. Parasitol Int 2004;53:293–9.
[38] Lim KC, Sun E, Bahgat M, Bucks D, Guy R, Hinz RS, et al. Blockage of skin invasion by schistosome cercariae by serine protease inhibitors. Am J Trop Med Hyg 1999;60:487–92.
[39] Basch PF. Cultivation of *Schistosoma mansoni* in vitro. I. Establishment of cultures from cercariae and development until pairing. J Parasitol 1981;67:179–85.
[40] Osada Y, Janecharut T, Hata H, Mahakunkij-Charoen Y, Chen XW, Nara T, et al. Protective immunity to *Schistosoma japonicum* infection depends on the balance of T helper cytokine responses in mice vaccinated with γ-irradiated cercariae. Parasite Immunol 2001;23:251–8.
[41] Boros DL, Warren KS. Delayed hypersensitivity-type granuloma formation and dermal reaction induced and elicited by a soluble factor isolated from *Schistosoma mansoni* eggs. J Exp Med 1970;32:488–507.
[42] Laemmli UK. Cleavage of structural proteins during the assembly of the head of bacteriophage T4. Nature 1970;227:680–5.
[43] Linke T, Ross AC, Harrison EH. Proteomic analysis of rat plasma by two-dimensional liquid chromatography and matrix-assisted laser desorption ionization time-of-flight mass spectrometry. J Chromatogr A 2006;1123:160–9.
[44] Delgado V, McLaren DJ. Evidence for enhancement of IgG1 subclass expression in mice polyvaccinated with radiation-attenuated cercariae of *Schistosoma mansoni* and the role of this isotype in serum-transferred immunity. Parasite Immunol 1990;12:15–32.
[45] Simpson AJG, James TSL, Sher A. Identification of surface antigens of Schistosomula of *Schistosoma mansoni* recognized by antibodies from mice immunized by chronic infection and by exposure to highly irradiated cercariae. Infect Immun 1983;41:591–7.
[46] Dalton JP, Strand M, Mangold BL, Dean DA. Identification of *Schistsoma mansoni* glycoprotein recognized by protective antibodies from mice immunized with irradiated cercariae. J Immunol 1986;136:4689–94.
[47] Cummings RD, Nyame AK. Glycobiology of schistosomiasis. FASEB J 1996;10:838–48.
[48] Cheng GF, Lin JJ, Feng XG, Fu ZQ, Jin YM, Yuan CX, et al. Proteomic analysis of differentially expressed proteins between the male and female worm of *Schistosoma japonicum* after pairing. Proteomics 2005;5:511–21.
[49] Simpson AJ, Sher A, McCutchan TF. The genome of *Schistosoma mansoni*: isolation of DNA, its size, bases and repetitive sequences. Mol Biochem Parasitol 1982;6:125–37.
[50] McManus DP, Hu W, Brindley PJ, Feng Z, Han Z-G. Schistosome transcriptone analysis at the cutting edge. Trends Parasitol 2004;20:301–4.
[51] Ashton PD, Curwen RS, Wilson RA. Linking proteome and genome: how to identify parasite proteins. Trends Parasitol 2001;17:198–202.
[52] Fernanda JC, Olavo SP, Camila SS, Renata G-Sá, Vanderlei R. *Schistosoma mansoni* encodes SMT3B and SMT3C molecules responsible for post-translational modification of cellular proteins. Parasitol Int 2008;57:72–178.
[53] Lee H-J, Lee E-Y, Kwon M-S, Paik Y-K. Biomarker discovery from the plasma proteome using multidimensional fractionation proteomics. Curr Opin Chem Biol 2006;10:42–9.

Available online at www.sciencedirect.com
ScienceDirect
Parasitology International 57 (2008) 54–61
www.elsevier.com/locate/parint

Change of subunit composition of mitochondrial complex II (succinate–ubiquinone reductase/quinol–fumarate reductase) in *Ascaris suum* during the migration in the experimental host

Fumiko Iwata [a,b], Noriko Shinjyo [a], Hisako Amino [a], Kimitoshi Sakamoto [a], M. Khyrul Islam [c], Naotoshi Tsuji [c], Kiyoshi Kita [a,*]

[a] *Department of Biomedical Chemistry, Graduate School of Medicine, The University of Tokyo, 7-3-1 Hongo, Bunkyo-ku, Tokyo 113 0033, Japan*
[b] *Department of Molecular and Cellular Physiology, Graduate School of Comprehensive Human Sciences, University of Tsukuba, Tsukuba, Japan*
[c] *Laboratory of Parasitic Diseases, National Institute of Animal Health, National Agriculture Research Organization, Tsukuba, Japan*

Received 13 July 2007; received in revised form 11 August 2007; accepted 16 August 2007
Available online 25 August 2007

Abstract

The mitochondrial metabolic pathway of the parasitic nematode *Ascaris suum* changes dramatically during its life cycle, to adapt to changes in the environmental oxygen concentration. We previously showed that *A. suum* mitochondria express stage-specific isoforms of complex II (succinate–ubiquinone reductase: SQR/quinol–fumarate reductase: QFR). The flavoprotein (Fp) and small subunit of cytochrome *b* (CybS) in adult complex II differ from those of infective third stage larval (L3) complex II. However, there is no difference in the iron–sulfur cluster (Ip) or the large subunit of cytochrome *b* (CybL) between adult and L3 isoforms of complex II. In the present study, to clarify the changes that occur in the respiratory chain of *A. suum* larvae during their migration in the host, we examined enzymatic activity, quinone content and complex II subunit composition in mitochondria of lung stage L3 (LL3) *A. suum* larvae. LL3 mitochondria showed higher QFR activity (~160 nmol/min/mg) than mitochondria of *A. suum* at other stages (L3: ~80 nmol/min/mg; adult: ~70 nmol/min/mg). Ubiquinone content in LL3 mitochondria was more abundant than rhodoquinone (~1.8 nmol/mg versus ~0.9 nmol/mg). Interestingly, the results of two-dimensional bule-native/sodium dodecyl sulfate polyacrylamide gel electrophoresis analyses showed that LL3 mitochondria contained larval Fp (Fp^L) and adult Fp (Fp^A) at a ratio of 1:0.56, and that most LL3 CybS subunits were of the adult form ($CybS^A$). This clearly indicates that the rearrangement of complex II begins with a change in the isoform of the anchor CybS subunit, followed by a similar change in the Fp subunit.

Keywords: *Ascaris suum* lung-stage L3 (LL3); Complex II; Quinone; NADH–fumarate reductase; Quinol–fumarate reductase (QFR); Oxidative stress

1. Introduction

During the life cycle of the parasitic nematode *Ascaris suum*, it transitions from aerobic to anaerobic metabolism in parallel with changes in the environmental oxygen concentration (Fig. 1) [1–6]. In aerobic metabolism, which is used by *A. suum* larvae during their development from fertilized egg to third stage larvae (L3), phosphoenolpyruvate (PEP) is converted to pyruvate by pyruvate kinase, and pyruvate is converted to CO_2 and H_2O via the tricarboxylic acid (TCA) cycle, generating a large amount of ATP by aerobic oxidative phosphorylation [7]. Adult *A. suum* worms, which live in a low-oxygen environment, use the anaerobic phosphoenolpyruvate carboxykinase (PEPCK)-

Abbreviations: Fp, flavoprotein subunit; Ip, iron–sulfur cluster subunit; CybL, large subunit of cytochrome *b*; CybS, small subunit of cytochrome *b*; Fp^L, larval Fp; Fp^A, adult Fp; $CybS^L$, larval CybS; $CybS^A$, adult CybS; L3, third stage larva; LL3, lung stage L3; SDH, succinate dehydrogenase; SQR, succinate–ubiquinone reductase; QFR, quinol–fumarate reductase; UQ, ubiquinone; dUQ, decyl UQ; RQ, rhodoquinone; dRQ, decyl RQ; HPLC, high performance liquid chromatography; BN-PAGE, blue-native polyacrylamide gel electrophoresis; SDS-PAGE, sodium dodecyl sulfate-PAGE; CBB, Coomassie brilliant blue.

* Corresponding author. Tel.: +81 3 5841 3526; fax: +81 3 5841 3444.
E-mail address: kitak@m.u-tokyo.ac.jp (K. Kita).

1383-5769/$ - see front matter © 2007 Elsevier Ireland Ltd. All rights reserved.
doi:10.1016/j.parint.2007.08.002

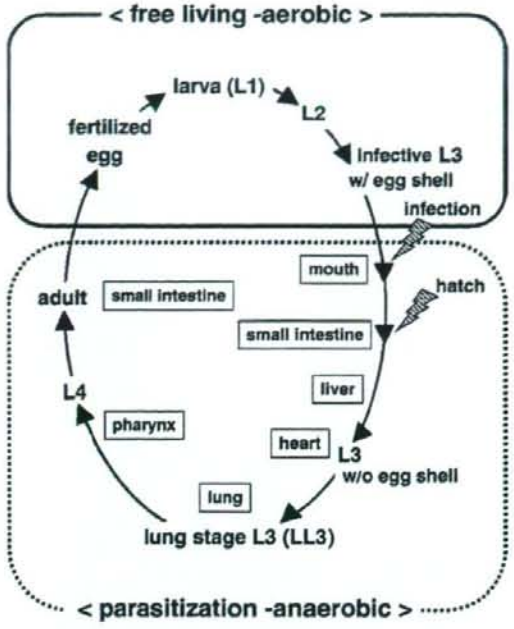

Fig. 1. Life cycle of *Ascaris suum*. Fertilized eggs grow to infective L3 under aerobic environment. Infective L3 larvae are ingested by the host, reach the small intestine and hatch there. Afterwards, larvae migrate into the host body (liver, heart, lung, pharynx), and finally migrate back to the small intestine and become adults. In the host small intestine, the oxygen concentration is only 2.5 to 5% of that of the exogenous environment [12]. w/, with; w/o, without.

succinate pathway. In the first step in the PEPCK-succinate pathway, PEPCK fixes CO_2 to PEP in the cytosol, to form oxaloacetate. This oxaloacetate is then reduced to malate, which is dismutated in mitochondria. Then, fumarate hydratase converts the malate to fumarate, which is reduced by the quinol–fumarate reductase (QFR) activity of complex II; in aerobic respiration, complex II catalyzes oxidation of succinate (succinate–ubiquinone reductase; SQR) in the mitochondria. The last step of the PEPCK-succinate pathway involves the NADH–fumarate reductase system, which is composed of complex I (NADH–quinone reductase), low-potential rhodoquinone (RQ) and complex II (QFR) [3,8]. Electron transfer from NADH to fumarate is coupled to ATP synthesis by site I phosphorylation in complex I. The difference in redox potential between NAD^+/NADH ($Em' = -320$ mV) and fumarate/succinate ($Em' = +30$ mV) is sufficient to drive ATP synthesis.

In eukaryotes, complex II is localized in the inner mitochondrial membrane, and is generally composed of 4 peptides [3]. The largest flavoprotein (Fp) subunit has an approximate molecular mass of 70 kDa and contains flavin adenine dinucleotide (FAD) as a prosthetic group. The relatively hydrophilic catalytic region of complex II is formed by the Fp subunit and the iron–sulfur cluster (Ip) subunit, whose molecular weight is about 30 kDa. The remaining subunits comprise cytochrome *b*, which contains heme *b*. Cytochrome *b* is composed of 2 hydrophobic membrane-anchoring polypeptide subunits; the 15-kDa large subunit (CybL) and the 13-kDa small subunit (CybS). These cytochrome *b* subunits are necessary for interaction between complex II and hydrophobic membrane-associated quinones such as ubiquinone (UQ) and RQ. However, it is unclear how heme *b* is involved in the electron transfer between complex II and quinones.

In a previous study, we showed that *A. suum* mitochondria express stage-specific isoforms of complex II [5,6,9]. While there is no difference in the isoforms of the Ip and CybL subunits of complex II between L3 larvae and adult *A. suum*, they have different isoforms of the complex II subunits Fp (larval, Fp^L; adult, Fp^A) and CybS (larval, $CybS^L$; adult, $CybS^A$). Quinone species in the mitochondria also change during the life cycle of *A. suum*. In adult mitochondria, the predominant quinone is the low-potential rhodoquinone (RQ; $Em' = -63$ mV); in larvae, the predominant quinone is ubiquinone (UQ; $Em' = +110$ mV) [10]. A combination of SQR and UQ, and that of QFR and a low-potential quinone, such as RQ or menaquinone (MK), is also observed in *E. coli* and other bacteria during metabolic adaptation to changes in oxygen supply [11]. UQ has a higher potential than RQ; therefore, RQ is better suited to transferring electrons to fumarate than is UQ. In L2 and L3 *A. suum* larvae, UQ preferentially donates electrons to the cytochrome chain in the mitochondria. Thus, UQ participates in aerobic metabolism in *A. suum* larvae, whereas RQ participates in anaerobic metabolism in adult *A. suum*.

After ingestion by the definitive host, the L3 larvae penetrate the intestinal wall and reach to the lung migrating through the tissues such as liver and heart. The L3 larvae passes from lung via the trachea to the small intestine where they molt to L4 and develop into sexually maturate adult worms in the small intestine [12]. Although studies have shown a clear difference in energy metabolism between larval and adult *A. suum* mitochondria, little is known about changes in the properties of mitochondria (including respiration) during migration of *A. suum* larvae in the host.

In the present study, we examined changes in subunit composition of *A. suum* larval complex II from lung stage L3 (LL3) larvae obtained from rabbits. Enzymatic analyses showed that properties of LL3 mitochondria differed from those of L3 and adult mitochondria. Protein chemical analysis revealed that the change in complex II begins with the anchor CybS subunit, and then occurs in the Fp subunit.

2. Materials and methods

2.1. Parasites

A. suum adult worms were procured from a slaughterhouse in Tokyo, Japan. Third stage infective (L3) larvae and lung stage L3 (LL3) larvae were obtained as previously described [5,13]. All animals used in this study were acclimatized to the experimental conditions for 2 weeks before the experiment. Animal experiments were conducted in accordance with the protocols approved by the Animal Care and Use Committee, National

Institute of Animal Health (Approval nos. 589,712). For the preparation of LL3 larvae, Japanese white rabbits were made to ingest infective *A. suum* eggs (approximately 1.5×10^5 eggs per rabbit), and infected lungs were removed from the rabbits 7 days after ingestion of the eggs. The lungs were cut into 2-cm cubes using a razor blade, and the cubes were put into nylon mesh bags (KA1000, Eiken Kizai, Tokyo, Japan) in 50-ml polypropylene conical tubes filled with phosphate-buffered saline (PBS) containing 100 μg/ml penicillin and 100 μg/ml streptomycin. Those tubes were then kept in a humidified incubator at 37 °C for 4 to 5 h. During that incubation, the larvae dropped out of the bags into the bottom of the tubes. The larvae were then washed several times with fresh PBS in a 37 °C water bath. Contaminating erythrocytes from the host rabbits were eliminated by hemolysis, which was induced by washing the pellet containing LL3 larvae with pre-warmed tap water at 37 °C. The body length of the LL3 larvae, obtained from infected rabbit on day 7 post-infection, were 1.2–1.3 mm. They were slightly smaller than LL3 larvae derived from infected swine at the same post-infectious stage (1.5 mm) [14].

2.2. Preparation of mitochondria from L3, LL3 and adult A. suum

Mitochondria from L3 and adult *A. suum* muscle were prepared using the method described by Amino et al. [5]. Because that method was not applicable to LL3 mitochondria, we established the following method to obtain active mitochondria from LL3; the entire procedure was performed on ice or at 4 °C. The LL3 larvae were gently suspended in an equal volume of ice-cold suspension buffer containing 210 mM mannitol, 10 mM sucrose, 1 mM disodium EDTA and 50 mM Tris–HCl (pH 7.5), supplemented with 10 mM sodium malonate [15]. The LL3 larvae in the suspension were cut using a scalpel (No. 10 blade, Feather, Osaka, Japan) on a 90 × 75 × 3-mm custom-made glass plate with a hollow (diameter, 22 mm; depth, 3 mm) in the middle. The cut larvae were then homogenized with a hand-powered glass–glass homogenizer for 15 min, and the homogenate was centrifuged at 500 × g for 1 min. The resulting supernatant was centrifuged at 10,000 × g for 10 min to obtain the mitochondrial pellet. The pellet was resuspended in the suspension buffer and stored at −80 °C until used. The protein concentration of the mitochondria was determined using the method of Lowry [16], using bovine serum albumin as the standard.

2.3. Enzyme assay

All assays were performed at 25 °C, using 50 mM potassium phosphate (pH 7.5) as the reaction buffer. The SQR [17], succinate dehydrogenase (SDH) [18], QFR [19] and NADH–fumarate reductase [8] activities of mitochondria were assayed as described. The NADH-decyl UQ (-dUQ) and NADH-decyl RQ (-dRQ) assays were performed using the same method as the NADH–fumarate reductase activity assay, except that 60 μM dUQ or dRQ was used as the electron acceptor, instead of sodium fumarate.

2.4. Quantitative analysis of quinone in LL3 mitochondria

Quinones were extracted from lyophilized LL3 mitochondria, and were analyzed by reverse-phase HPLC as described by Miyadera et al. [20]. The concentrations of quinones were determined spectrophotometrically using the following extinction coefficients: for UQ, $E_{1\%1\ cm}$ at 275 nm = 158; for RQ, $E_{1\%1\ cm}$ at 283 nm = 141 [10].

2.5. Western blotting

Complex II from L3, LL3 and adult mitochondria was analyzed by Western blotting using the method of Towbin et al. [21]. The mitochondrial proteins were separated by SDS-PAGE, using a 7.5% acrylamide gel for the Fp subunit, and using a 10/20% gradient acrylamide gel (Daiichi, Tokyo, Japan) for the Ip and CybS subunits. The proteins were then transferred to a nitrocellulose membrane at 4 °C and 80 V for 1 h. The membranes were incubated with the following antibodies in Tris-buffered saline containing 0.05% (w/v) Tween 20 (TBST) and 2% (w/v) skim milk: anti-Fp monoclonal, diluted 1:3000 [18]; anti-CybS^A monoclonal, diluted 1:5000 [5]; CybS^L peptide-based polyclonal, diluted 1:300 [5]; mixture of anti-Ip and anti-CybS polyclonal, diluted 1:2000 [5]. Each membrane was then incubated for 30 min with one of the following alkaline phosphatase-conjugated secondary antibodies: goat anti-mouse IgG (for Fp and CybS^A), or goat anti-rabbit IgG (for CybS^L, Ip and CybS). The proteins were detected using the alkaline phosphatase method. The amount of protein was normalized to the intensity of the Ip subunit at each stage, using NIH Image (a free image analyzing program for the Macintosh, developed by National Institutes of Health (NIH); www.rsb.info.nih.gov/nih-image/download.html).

2.6. Solubilization of mitochondria for blue native (BN-) PAGE

Mitochondria from L3, LL3 and adult *A. suum* (1.5 μmol/min in SDH activity) were incubated on ice for 1 h in 0.5% (w/v) sucrose monolaurate (SML) and Native PAGE™ sample buffer containing 50 mM Bis–Tris, 6 N HCl, 50 mM NaCl, 10% (w/v) glycerol and 0.001% (w/v) Ponceau S in 10 mM Tris–HCl (pH 7.5) (User manual, version A 2006; www.invitrogen.com/content/sfs/manuals/nativepage_man.pdf, Invitrogen, Carlsbad, CA, USA). They were then ultracentrifuged at 200,000 × g and 4 °C for 1 h, and the resulting supernatant was subjected to BN-PAGE, as described below.

2.7. BN-PAGE, CBB staining, in-gel SDH activity staining and Western blotting

The solubilized mitochondria were subjected to BN-PAGE [22] using Native PAGE Novex 4–16% Bis–Tris gels (Invitrogen). Electrophoresis was performed at 4 °C, at 150 V for 1 h, and then at 250 V, voltage constant. The cathode and anode buffers were prepared according to the user's manual of the Native PAGE Novex Bis–Tris gel system. Following the BN-PAGE, CBB staining was performed according to the user's

manual. The SDH activity of mitochondrial protein of L3, LL3 and adult *A. suum* was detected as described elsewhere [18,23]. After the BN-PAGE (first dimension), the gel cut by lane from the first-dimensional gel was equilibrated with SDS-PAGE buffer, and was then loaded onto the second-dimensional gel (7.5% acrylamide gel for Fp, and 10/20% gradient acrylamide gels (Daiichi) for Ip and CybS). The subsequent analysis by Western blotting was performed as described above.

3. Results

3.1. Enzymatic properties of LL3 complex II

Because only a small amount of LL3 larvae was obtained, and because LL3 larvae were more resistant to homogenization than L3 larvae and adult worms, we tried to establish a specific and reproducible protocol for the preparation of mitochondria from LL3 larvae. We found that cutting LL3 larvae with a scalpel was an effective method of recovering active mitochondria. Using the established protocol, we obtained approximately 0.5 mg of mitochondria from 1 infected rabbit. Fig. 2 shows the results of comparative analysis of enzyme activities, relative to NADH–fumarate reductase activity, in L3, LL3 and adult mitochondria.

The Fp and Ip subunits form the hydrophilic catalytic portion of complex II, and act as a succinate dehydrogenase (SDH), catalyzing the oxidation of succinate by the water-soluble electron acceptor phenazine methosulfate. The L3 and LL3 mitochondria had almost identical levels of SDH activity, whereas the SDH activity of adult mitochondria was 2.7 to 3.9 times higher than that of L3 and LL3 mitochondria (Fig. 2A). SQR catalyzes electron transfer from succinate to the physiological electron acceptor, ubiquinone. Similarly, SQR activity of adult mitochondria was 1.8 to 3.9 times higher than that of L3 and LL3 mitochondria (Fig. 2B). QFR catalyzes a reaction that is the reverse of the reaction catalyzed by SQR. The QFR activity of LL3 mitochondria was higher than that of L3 and adult mitochondria (Fig. 2C). The NADH–fumarate

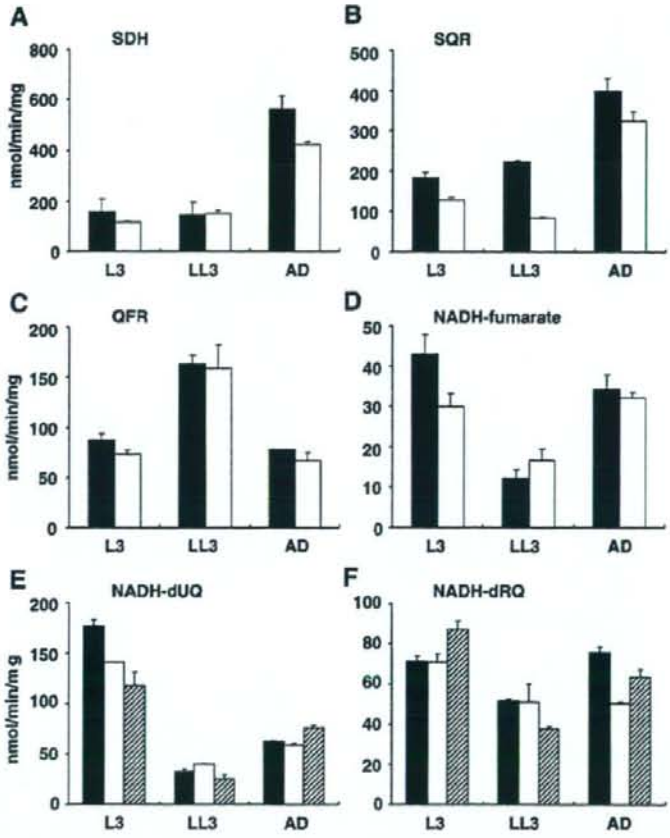

Fig. 2. Enzyme assay. Enzyme activities of complex I and II of mitochondria from L3 *A. suum* larvae, LL3 *A. suum* larvae, and *A. suum* adults. (A) SDH, (B) SQR, (C) QFR, (D) NADH–fumarate reductase, (E) NADH-dUQ and (F) NADH-dRQ. The mean and standard error were derived from triplicate measurements. Solid bars indicate experiment 1; open bars indicates experiment 2; stripe bars indicate experiment 3. Assays were performed as in materials and methods.

reductase system is an anaerobic electron-transport system of mitochondria, and is the terminal step of the PEPCK-succinate pathway. In the NADH–fumarate reductase system, the reducing equivalent of NADH is transferred to the low-potential RQ by the NADH-RQ reductase complex (Complex I). This pathway ends with the production of succinate by the rhodoquinol-fumarate reductase activity of complex II. Unexpectedly, the NADH–fumarate reductase activity of LL3 mitochondria was lower than that of L3 and adult mitochondria (Fig. 2D). The NADH-dUQ and NADH-dRQ activities of LL3 mitochondria were lower than those of L3 and adult mitochondria (Fig. 2E and F), suggesting that the low NADH–fumarate reductase activity of LL3 mitochondria is due to the lower activity of complex I in LL3 mitochondria.

3.2. Quinone components in LL3 mitochondria

Because quinone species are important low-molecular-weight mediators of electron transfer between respiratory enzymes, and because the ratio between RQ and UQ seems to be a critical factor in the direction of electron transfer in the chain, we examined the quinone content of LL3 mitochondria complex II. Although the amount of LL3 mitochondria that we obtained was quite limited, we performed the analysis using 2 different samples of LL3 mitochondria. The first sample of LL3 mitochondria contained 1.68 nmol/mg UQ-9 and 0.85 nmol/mg RQ-9. A similar result was obtained for the second sample (Table 1), indicating that the UQ content of LL3 mitochondria is approximately 2-fold greater than that of RQ. It should be noted that UQ-9 is the predominant quinone of L3 complex II (75% of the total quinone content), and that RQ is the only quinone present in complex II from adult *A. suum* muscle [10].

3.3. Subunit composition of the LL3 mitochondria complex II

To examine the subunit structure of complex II in LL3 mitochondria, we performed Western blotting. Because the isoforms of the Ip and CybL subunits do not change during the *A. suum* life cycle [5], the amount of proteins used for the Western blotting of Fp and CybS subunits was normalized to the intensity of the Ip subunit, which was visualized using the alkaline phosphatase method (Fig. 3D). LL3 mitochondrial complex II contained both Fp^L and Fp^A (Fig. 3). The LL3 and adult complex II had a Fp^L:Fp^A band intensity ratio of 1:0.56 and 1:3.5, respectively, whereas only the Fp^L band was observed in blots of L3 complex II (Fig. 3A). For the $CybS^A$ subunit, the

Table 1
Quinone quantitative analysis of LL3 mitochondria

Experiment	(nmol/mg) UQ-9[a]	RQ-9[b]	Ratio UQ-9[a]:RQ-9[b]
1	1.68	0.85	1.98:1
2	1.89	1.00	1.89:1

[a] UQ-9, ubiquinone-9.
[b] RQ-9, rhodoquinone-9.

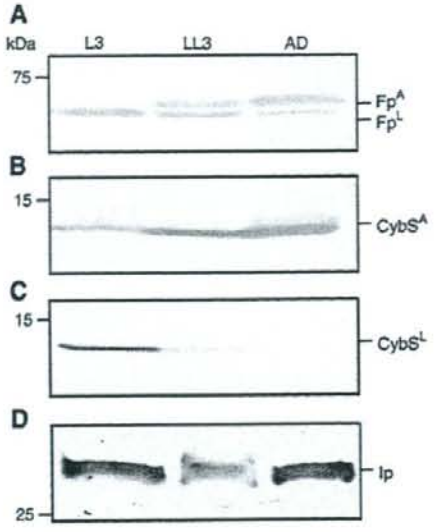

Fig. 3. Western blotting. Western blotting with (A) *A. suum* Fp monoclonal antibody, diluted 1:3000. (B) Monoclonal antibody against $CybS^A$ diluted 1:5000, and (C) Peptide-based polyclonal antibody against $CybS^L$ diluted 1:300. Protein levels were normalized to the Ip band intensity using (D) mixture of anti-Ip and anti-CybS polyclonal antibody diluted 1:2000. L3, *A. suum* larvae prepared from embryonated eggs; LL3, lung-stage L3; AD, *A. suum* adult. Precision Plus All Blue Standard (BIO-RAD).

L3:LL3:adult band intensity ratio was 1:3.5:6.1 (Fig. 3B). Only a small amount of $CybS^L$ was detected in LL3 mitochondria (<5% of $CybS^L$ in L3 mitochondria), and no $CybS^L$ was found in adult mitochondria (Fig. 3C). This result was reproducible in more than 3 experiments, suggesting that the subunit isoform change of LL3 complex II starts with CybS, and then occurs in Fp.

Because Western blotting clearly showed a difference in timing of isoform change between Fp and CybS subunits during migration in the host, we used BN-PAGE to examine the subunit composition of functional complex II. Mitochondrial proteins of each stage solubilized with sucrose monolaurate were subjected to BN-PAGE, and were then stained for CBB (Fig. 4A) or SDH activity (Fig. 4B) in the gel. Complex II from all 3 stages exhibited SDH activity in the gel, and band intensities of the 3 stages were almost identical when the amount of protein was normalized to 1.5 μmol/min SDH activity.

Next, we performed two-dimensional electrophoresis; with BN-PAGE as the first dimension, and SDS-PAGE as the second dimension. After the BN-PAGE, the gel was cut and was horizontally loaded onto SDS-PAGE. Following the two-dimensional electrophoresis, proteins were analyzed by Western blotting (Fig. 4C). Spots of Fps and CybSs were found in the same position as the SDH-stain band, indicating that native complex II with 4 subunits migrated during electrophoresis in the presence of the detergent. No extra spot was found in an area different from the SDH-stain position. In addition, the patterns

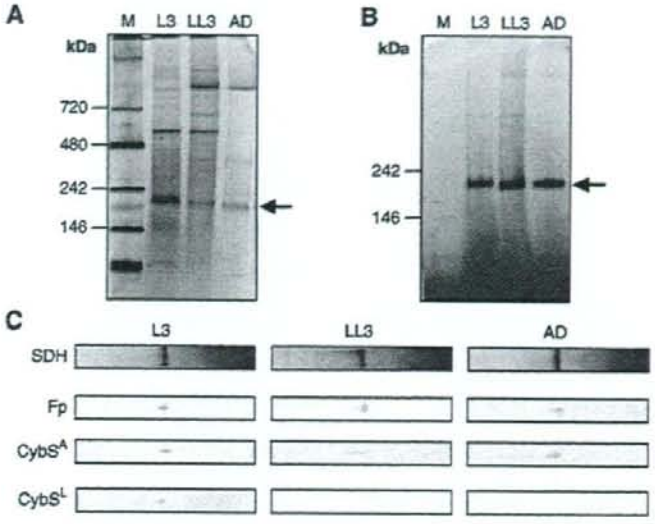

Fig. 4. BN-PAGE analysis. BN-PAGE analysis of mitochondria from *A. suum* L3 larvae, LL3 larvae and adults (1.5 μmol/min SDH activity). (A) CBB-stain. Arrow indicates expected SDH active bands. (B) SDH activity stained in gels of Native PAGE™ Bis–Tris gel (4–16%). Arrow shows SDH active bands. (C) Western blotting after SDS-PAGE, following BN-PAGE. Antibodies used were the same as in Fig. 3. The size marker is Native Mark Unstained Protein Standard (Invitrogen).

of intensity of the spots in Fig. 4C were almost identical to the results of Western blotting after SDS-PAGE (Fig. 3).

4. Discussion

In the present study, biochemical analyses of mitochondrial complex II were performed to elucidate how complex II in *A. suum* mitochondria change its isoform composition during migration in the mammalian host. In the first step of this study, we examined complex II from LL3 larvae (Fig. 1), because there is an established method of sample collection from rabbit lung, and because several properties of LL3 have been well studied [13,24]. The natural host of *A. suum* is swine so that we need pigs for developing the migratory phase and the adult stages. However, pig rearing facilities are currently quite limited for the purpose of doing *Ascaris* infection. Helminth researchers have previously examined the life cycle and worm burdens in rabbits [25,26]. The results showed that several criteria such as the organ migratory routes and recovery of larvae in rabbits were quite similar to those in pigs, indicating that rabbit can be fairly used for permissive hosts. Actually, *Ascaris* researchers including our group have employed rabbits to do biochemical experiments of the roundworms [27,28].

We previously demonstrated that *A. suum* mitochondria express stage-specific isoforms of complex II; i.e., the flavoprotein subunit (Fp) and the small subunit of cytochrome *b* (CybS) of complex II isolated from L3 infective eggs differ from those of adult muscle complex II, while the 2 forms of complex II have an identical iron-sulfur cluster subunit (Ip) and large subunit of cytochrome *b* (CybL). Therefore, the subunit isoform composition of complex II must change during migration in the host. To our surprise, Western blot analyses showed that both the Fp^L and Fp^A isoforms (in the ratio of 1: 0.56) were present in LL3 mitochondria, while the majority of CybS subunit was of the isoform $CybS^A$ (Fig. 3A and B). This means that expression of adult Fp does not synchronize with that expression of adult CybS, and suggests that LL3 complex II has a different combination of subunit isoforms than L3 and adult complex II.

To analyze the native state of complex II subunit composition in LL3 mitochondria, we used BN-/SDS-PAGE two-dimensional electrophoresis (Fig. 4C). The spots of the subunits were found at the same position as the SDH bands,

Table 2
Enzyme activities of L3, LL3 and adult complex I and II of *Ascaris suum* mitochondria

		Specific activity (nmol/min/mg)		
Assay	Experiment	L3	LL3	Adult
SDH	1	158±36	145±16	566±15
(complex II)	2	118±5.6	152±25	424±22
SQR	1	184±28	224±8.3	400±63
(complex II)	2	129±16	84.1±4.0	326±43
QFR	1	87.8±6.0	164±8.6	78.5±0.058
(complex II)	2	73.5±7.6	159±47	66.8±16
NADH–fumarate	1	43.0±10	12.3±4.4	34.4±7.1
reductase (complex I,II)	2	30.1±6.4	16.7±5.6	32.3±2.6
NADH-dUQ	1	177±12	32.3±5.6	62.4±1.9
	2	141±0.92	39.8±1.9	58.6±4.6
(complex I)	3	118±26	24.8±8.8	76.3±4.9
NADH-dRQ	1	71.4±4.4	51.6±2.0	75.7±5.6
	2	71.0±7.8	51.0±18	50.3±1.3
(complex I)	3	87.1±8.5	37.6±2.4	63.4±7.6

without any extra spots. This result indicates that the spots detected were derived from active complex II consisting of 4 subunits. In LL3 mitochondria, all 4 larva-/adult-types of Fp-CybS subunits was observed, while Fp^L, $CybS^A$ and $CybS^L$ subunit isoforms were detected in L3 mitochondria, and Fp^L, Fp^A and $CybS^A$ subunit isoforms were detected in adult mitochondria. The pattern of the intensity of the spots in Fig. 4C is consistent with that of the Western blotting after SDS-PAGE (Fig. 3), indicating that mitochondrial complex II subunit switching first occurs in CybS, and then occurs in Fp, during migration in the host.

Of the 4 possible Fp-CybS subunit combinations (Fp^L-$CybS^A$, Fp^A-$CybS^A$, Fp^L-$CybS^L$ and Fp^A-$CybS^L$), Fp^L-$CybS^A$ is the predominant combination in LL3 mitochondria. Western blot analysis of young adult mitochondria obtained from the muscle of 12-cm-long female worms showed that $CybS^L$ had completely disappeared, whereas Fp^L remained at a ratio of Fp^L:Fp^A = 1:1.5 (data not shown), although only 1 SDH band was observed in BN-PAGE. This finding may be due to similar properties between the 2 complexes with different combinations.

However, several questions remain unanswered. Because of limited sample amount, it is difficult to purify complex II from LL3 mitochondria. Reports indicate that adult *A. suum* uses the NADH–fumarate reductase system in its anaerobic host environment; in the NADH–fumarate reductase system, the QFR activity of mitochondrial complex II plays a significant role [3,29,30]. However, we previously found that L3 complex II had higher QFR activity than adult complex II, and presumed that this was due to pre-adaptation to the dramatic change in oxygen availability during infection of the host [5]. In the present study, we found that the QFR activity of LL3 complex II was twice as high as that of L3 complex II (Fig. 2C, Table 2). The host lung is a relatively aerobic environment (13.2% O_2) [31], suggesting that the larvae pre-adapt before they migrate into the anaerobic environment of the host small intestine (5% O_2).

Although LL3 mitochondria showed the highest QFR activity of the 3 stages we examined, their NADH–fumarate reductase activity was unexpectedly low (Fig. 2D). This appears to be due to the effects of low complex I activity, as indicated by the NADH-dUQ and NADH-dRQ assays (Fig. 2E and F). The NADH–fumarate reductase system is composed of complex I (initial dehydrogenase of NADH), RQ (electron mediator), and complex II (terminal oxidase for fumarate reduction). We also examined the quinone content of the mitochondria. Analysis of the quinone contents of mitochondria isolated from unembryonated eggs, L3 larvae and adult muscle showed that the predominant quinone in larval mitochondria (which possess an aerobic respiratory chain) was UQ-9 (75% of the total quinone content) [10]. In contrast, the only quinone present in anaerobic mitochondria from adult muscle is RQ-9. Consistent with these findings, reconstitution studies using bovine heart complex I and adult *A. suum* QFR show that RQ is essential for the function of the NADH–fumarate reductase system [32]. Specifically, when RQ-9 was incorporated into the system, the maximum activity of reconstituted NADH–fumarate reductase activity was 430 nmol/min/mg of *A. suum* complex II, while no activity was observed in the presence of UQ-9. In addition, our previous findings suggest that although *A. suum* adult complex I uses both RQ and UQ as electron acceptors, the 2 quinones have different ways of binding reaction and reaction with *A. suum* complex I [33]. It should be noted that in the present study, UQ accounted for 66% of the total quinone of LL3 complex II, which is an intermediate between those of L3 and adult complex II [10]. Further analysis of the effect of endogenous quinones in the mitochondria of the enzyme activities of complex I and complex II is needed to elucidate the unique properties of the NADH–fumarate reductase system of *A. suum*.

In the present study, we examined how mitochondrial complex II of *A. suum* changes its subunit composition, especially during migration in the host. We found that the small subunit of cytochrome *b* (CybS) starts to change its isoform before the flavoprotein (Fp) subunit does so. Further clarification of this process will require analysis of larvae from other migration stages in the host. In each stage, the metabolic pathway of *A. suum* may continue to change according to the environmental changes, even in the host body. To elucidate this dynamic change in the mitochondrial respiratory system of *A. suum* during migration, we plan to establish an experimental system using swine, which is a definitive host of *A. suum*. With such a system, further biochemical analysis should reveal novel properties of complex II in LL3 mitochondria.

Acknowledgements

We thank Dr. Tetsuro Ishii for his academic support. This study was supported by a grant-in-aid for scientific research on Priority Areas, for the 21st Century COE Program (F-3) and for Creative Scientific Research from the Japanese Ministry of Education, Science, Culture, Sports and Technology (180 73004, 18GS0314).

References

[1] Komuniecki R, Komuniecki PR. Aerobic–anaerobic transitions in energy metabolism during the development of the parasitic nematode *Ascaris suum*. In: Boothroyd JC, Komuniecki R, editors. Molecular approaches to parasitology. New York: Wiley-Liss; 1995.

[2] Tielens AGM, Rotte C, van Hellemond JJ, Martin W. Mitochondria as we don't know them. Trends Biochem Sci 2002;27:56–72.

[3] Kita K, Takamiya S. Electron-transfer complexes in *Ascaris* mitochondria. Adv Parasitol 2002;51:95–131.

[4] Kita K. Electron-transfer complexes in *Ascaris suum*. Parasitol Today 1992;8: 155–9.

[5] Amino H, Osanai A, Miyadera H, Shinjyo N, Tomitsuka E, Taka H, et al. Isolation and characterization of the stage-specific cytochrome *b* small subunit (CybS) of *Ascaris suum* complex II from the aerobic respiratory chain of larval mitochondria. Mol Biochem Parasitol 2003;128: 175–86.

[6] Amino H, Wang H, Hirawake H, Saruta F, Mizuchi D, Mineki R, et al. Stage-specific isoforms of *Ascaris suum* complex II: the fumarate reductase of the parasitic adult and the succinate dehydrogenase of free-living larvae share a common iron–sulfur subunit. Mol Biochem Parasitol 2000;106: 63–76.

[7] Kita K, Hirawake H, Miyadera H, Amino H, Takeo S. Role of complex II in anaerobic respiration of the parasite mitochondria from *Ascaris suum* and *Plasmodium falciparm*. Biochim Biophys Acta 2002;1553: 123–39.

[8] Omura S, Miyadera H, Ui H, Shiomi K, Yamaguchi Y, Masuma R, et al. An anthelmintic compound, nafredin, shows selective inhibition of

complex I in helminth mitochondria. Proc Natl Acad Sci U S A 2001;98: 60–2.
[9] Saruta F, Kuramochi T, Nakamura K, Takamiya S, Yu Y, Aoki T, et al. Stage-specific isoforms of complex II (succinate–ubiquinone oxidoreductase) in mitochondria from the parasitic nematode, *Ascaris suum*. J Biol Chem 1995;270:928–32.
[10] Takamiya S, Kita K, Wang H, Weinstein PP, Hiraishi A, Oya H, et al. Developmental changes in the respiratory chain of *Ascaris* mitochondria. Biochim Biophys Acta 1993;1141:65–74.
[11] Cole ST, Condon C, Lemire BD, Weiner JH. Molecular biology, biochemistry and bioenergetics of fumarate reductase, a complex membrane-bound iron-sulfur flavoenzyme of *Escherichia coli*. Biochim Biophys Acta 1985;811: 381–403.
[12] Heinz M. Encyclopedic reference of parasitology. 2nd ed. Berlin: Springer; 2001.
[13] Islam MK, Miyoshi T, Yamada M, Alim MA, Huang X, Motobu M, et al. Effect of piperazine (diethylenediamine) on the moulying proteome express and pyrophosphate activity of *Ascaris suum* lung-stage larvae. Acta Trop 2006;99:208–17.
[14] Miyazaki I. Helminthic zoonoses. Tokyo: International Medical Foundation of Japan; 1991. p. 295–305.
[15] Takamiya S, Furushima R, Oya H. Electron transfer complexes of *Ascaris suum* muscle mitochondria I. Characterization of NADH-cytochrome *c* reductase (complex I–III), with special reference to cytochrome localization. Mol Biochem Parasitol 1984;13: 121–34.
[16] Lowry OH, Rosebrough NJ, Farr AL, Randall RJ. Protein measurement with the folin phenol reagent. J Biol Chem 1951;193:265–75.
[17] Miyadera H, Shiomi K, Ui H, Yamaguchi Y, Masuma R, Tomoda H, et al. Atopenins, potent and specific inhibitors of mitochondrial complex II (succinate–ubiquinone oxidoreductase). Proc Natl Acad Sci U S A 2003;100: 473–7.
[18] Tomitsuka E, Goto Y, Taniwaki M, Kita K. Direct evidence for expression of Type II flavoprotein subunit in human complex II (succinate–ubiquinone reductase). Biochem Biophys Res Commun 2003;311: 774–9.
[19] Kita K, Vibat CR, Meinhardt S, Guest JR, Gennis RB. One-step purification from *Escherichia coli* of complex II (succinate:ubiquinone oxidoreductase) associated with succinate-reducible cytochrome b_{556}. J Biol Chem 1989;264:2672–7.
[20] Miyadera H, Amino H, Hiraishi A, Taka H, Murayama K, Miyoshi H, et al. Altered quinone biosynthesis in the long-lived *clk-1* mutants of *Caenorhabditis elegans*. J Biol Chem 2001;276:7713–6.
[21] Towbin H, Staehelin T, Gorton J. Electrophoretic transfer of proteins from polyacrylamide gels to nitrocellulose sheets: procedure and some applications. Proc Natl Acad Sci U S A 1979;76: 4350–4.
[22] Shägger H, Cramer WA, von Jagow G. Analysis of molecular mass and oligomeric states of protein complexes by blue native electrophoresis and isolation of membrane protein complexes by two-dimensional native electrophoresis. Anal Biochem 1994;217:220–30.
[23] Kho CW, Park SG, Lee DH, Cho S, Oh GT, Kang S, et al. Activity staining of glutathione peroxidase after two-dimensional gel electrophoresis. Mol Cell 2004;18:369–73.
[24] Geenen PL, Bresciani J, Boes J, Pedersen A, Eriksen L, Fagerholm HP, et al. The morphogenesis of *Ascaris suum* to the infective third-stage larvae within the egg. J Parasitol 1999;85:616–22.
[25] Jeska EL, Williams JF, Cox DF. *Ascaris suum*: larval returns in rabbits, Guinea pigs and mice after low-dose exposure to eggs. Exp Parasitol 1969;26: 187–92.
[26] Stormberg BE, Soulsby EJL. *Ascaris suum*: immunization with soluble antigens in the Guinea pig. Int J Parasitol 1977;7:287–91.
[27] Komuniecki PR, Vanover L. Biochemical changes during the aerobic–anaerobic transition in *Ascaris suum* larvae. Mol Biochem Parasitol 1987;22(2–3):241–8.
[28] Islam MK, Miyoshi T, Kasuga-Aoki H, Isobe T, Arakawa Y, Matsumoto Y, et al. Inorganic pyrophosphatase in the roundworm *Ascaris* and its role in the development and molting process of the larval stage parasites. Eur J Biochem 2003;270: 2814–26.
[29] Kita K, Shiomi K, Omura S. Advances in drug discovery and biochemical studies. Trends Parasitol 2007;23:223–9.
[30] Kuramochi T, Hirawake H, Kojima S, Takamiya S, Furushima R, Aoki T, et al. Sequence comparison between the flavoprotein subunit of the fumarate reductase (complex II) of the anaerobic parasitic nematode, *Ascaris suum* and the succinate dehydrogenase of the aerobic, free-living nematode, *Caenorhabditis elegans*. Mol Biochem Parasitol 1994;68: 177–87.
[31] Martini FH, Ober WC, Garrison CW, Welch K, Hutching RT. Fundamentals of anatomy and physiology. 4th ed. Upper Saddle River, New Jergy: Prentice Hall; 1998.
[32] Kita K, Takamiya S, Furushima R, Ma YC, Suzuki H, Ozawa T, et al. Electron-transfer complexes of *Ascaris suum* muscle mitochondria. III. Composition and fumarate reductase activity of complex II. Biochim Biophys Acta 1998;935: 130–40.
[33] Yamashita T, Ino T, Miyoshi H, Sakamoto K, Osanai A, Nakamaru-Ogiso E, et al. Rhodoquinone reaction site of mitochondrial complex I, in parasitic helminth, *Ascaris suum*. Biochim Biophys Acta 2004;1608: 97–103.

ANTIMICROBIAL AGENTS AND CHEMOTHERAPY, Jan. 2008, p. 164–170
0066-4804/08/$08.00+0 doi:10.1128/AAC.00378-07

Vol. 52, No. 1

Anaerobic NADH-Fumarate Reductase System Is Predominant in the Respiratory Chain of *Echinococcus multilocularis*, Providing a Novel Target for the Chemotherapy of Alveolar Echinococcosis▽

Jun Matsumoto,[1] Kimitoshi Sakamoto,[2]* Noriko Shinjyo,[2] Yasutoshi Kido,[2] Nao Yamamoto,[1] Kinpei Yagi,[3] Hideto Miyoshi,[4] Nariaki Nonaka,[1] Ken Katakura,[1] Kiyoshi Kita,[2] and Yuzaburo Oku[1]

Laboratory of Parasitology, Department of Disease Control, Graduate School of Veterinary Medicine, Hokkaido University, Sapporo, Japan[1]; Department of Biomedical Chemistry, Graduate School of Medicine, University of Tokyo, Tokyo, Japan[2]; Department of Medical Zoology, Hokkaido Institute of Public Health, Sapporo, Japan[3]; and Division of Applied Life Sciences, Graduate School of Agriculture, Kyoto University, Kyoto, Japan[4]

Received 20 March 2007/Returned for modification 21 June 2007/Accepted 10 October 2007

Alveolar echinococcosis, which is due to the massive growth of larval *Echinococcus multilocularis*, is a life-threatening parasitic zoonosis distributed widely across the northern hemisphere. Commercially available chemotherapeutic compounds have parasitostatic but not parasitocidal effects. Parasitic organisms use various energy metabolic pathways that differ greatly from those of their hosts and therefore could be promising targets for chemotherapy. The aim of this study was to characterize the mitochondrial respiratory chain of *E. multilocularis*, with the eventual goal of developing novel antiechinococcal compounds. Enzymatic analyses using enriched mitochondrial fractions from *E. multilocularis* protoscoleces revealed that the mitochondria exhibited NADH-fumarate reductase activity as the predominant enzyme activity, suggesting that the mitochondrial respiratory system of the parasite is highly adapted to anaerobic environments. High-performance liquid chromatography–mass spectrometry revealed that the primary quinone of the parasite mitochondria was rhodoquinone-10, which is commonly used as an electron mediator in anaerobic respiration by the NADH-fumarate reductase system of other eukaryotes. This also suggests that the mitochondria of *E. multilocularis* protoscoleces possess an anaerobic respiratory chain in which complex II of the parasite functions as a rhodoquinol-fumarate reductase. Furthermore, in vitro treatment assays using respiratory chain inhibitors against the NADH-quinone reductase activity of mitochondrial complex I demonstrated that they had a potent ability to kill protoscoleces. These results suggest that the mitochondrial respiratory chain of the parasite is a promising target for chemotherapy of alveolar echinococcosis.

Echinococcosis is a near-cosmopolitan zoonosis caused by helminthic parasites belonging to the genus *Echinococcus* (family Taeniidae) (18). The life cycle of *Echinococcus* spp. includes an egg-producing adult stage in the definitive hosts and a larval stage in intermediate hosts including humans. The larval stage of the parasite produces a large number of infective protoscoleces that develop to adult worms after being ingested by the definitive host, or they produce a new parasite mass when liberated inside the intermediate host, causing metastases of the parasite lesions. The two major species of medical and public health importance are *Echinococcus granulosus* and *E. multilocularis*, which cause cystic echinococcosis and alveolar echinococcosis (AE), respectively.

Human AE is a life-threatening disease, and without careful clinical management, it has a high fatality rate and poor prognosis. Humans acquire AE infection by ingesting eggs from adult parasitic worms. Early diagnosis and treatment (mainly by radical surgery) of human AE are difficult because the disease progresses slowly and usually takes more than several years before clinical symptoms become apparent. An efficient chemotherapeutic compound is still not available. The first choice for the chemotherapy of AE is benzimidazole derivatives (18), but they are parasitostatic rather than parasitocidal against larval *E. multilocularis*. Therefore, the development of highly effective antiechinococcal drugs is urgently needed.

Biological systems for energy metabolism are essential for the survival, continued growth, and reproduction of all living organisms. "Typical" mitochondria are usually considered to be oxygen-consuming, ATP-producing organelles. In fact, typical mitochondria, such as those found in mammalian cells, require oxygen to function. They use pyruvate dehydrogenase for oxidative decarboxylation of pyruvate to acetyl coenzyme A, which is then completely oxidized to CO_2 through the Krebs cycle. Most of the energy is produced by oxidative phosphorylation: the electrons from NADH and succinate are transferred to oxygen by the proton-pumping electron transfer respiratory chain in which ubiquinone (UQ) (Fig. 1A) is commonly used as an electron mediator. The backflow of the protons results in ATP formation by the mitochondrial ATP synthase.

In parasitic organisms, on the other hand, the carbohydrate and energy metabolic pathways of adult parasitic helminths differ greatly from those of their vertebrate hosts. The most important factors in this respect are the nutrient and oxygen supply (reviewed in references 4, 12, and 13). Parasitic hel-

* Corresponding author. Mailing address: Department of Biomedical Chemistry, Graduate School of Medicine, University of Tokyo, Tokyo 113-0033, Japan. Phone: 81 3 58418202. Fax: 81 3 58413444. E-mail: sakamok@m.u-tokyo.ac.jp.

▽ Published ahead of print on 22 October 2007.

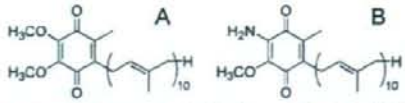

FIG. 1. Chemical structure of ubiquinone-10 (UQ_{10}) ($E_m' = +110$ mV) (A) and rhodoquinone-10 (RQ_{10}) ($E_m' = -63$ mV) (B).

minths have exploited a variety of energy-transducing systems during their adaptation to habitats in their hosts (7, 28). The parasitic nematode *Ascaris suum*, for example, resides in the host small intestine, where oxygen tensions are low, and exploits a unique anaerobic respiratory chain, called the NADH-fumarate reductase system, to adapt to its microaerobic habitat (Fig. 2) (2, 3, 14, 22; reviewed in reference 10). The NADH-fumarate reductase system is part of the unique respiratory system for parasitic helminthes and is the terminal step in the phosphoenolpyruvate carboxykinase-succinate pathway, which is found in many anaerobic organisms. Electrons from NADH are accepted by rhodoquinone (RQ) (Fig. 1B) via the NADH-RQ reductase activity of mitochondrial complex I and then transferred to fumarate through the rhodoquinol-fumarate reductase activity of mitochondrial complex II. The anaerobic electron transfer in complex I couples with proton transport across the mitochondrial inner membrane, providing ATP even in the absence of oxygen. This system, which does not normally function in mammalian mitochondria, is considered to be a good target for the development of novel anthelminthics (8, 9, 21). With regard to *Echinococcus* spp., the presence of both aerobic and anaerobic respiratory systems was previously suggested by a series of intensive studies (1, 16, 17), although the respiratory systems in this group of parasites are to be characterized in more detail.

In the present study, we prepared an enriched mitochondrial fraction from *E. multilocularis* protoscoleces and characterized the specific enzyme activities involved in mitochondrial energy metabolism as well as the quinone profile in the parasite's respiratory chain. Furthermore, based on findings reported previously by Yamashita et al. that quinazoline derivatives can inhibit the NADH-quinone reductase of mitochondria from *A. suum* (35), we tested several quinazoline-type compounds, with a view to developing novel antiechinococcal compounds.

MATERIALS AND METHODS

Isolation of *E. multilocularis* protoscoleces. We used the Nemuro strain of *E. multilocularis*, which is maintained at the Hokkaido Institute of Public Health (Sapporo, Japan). Mature larval parasites with protoscolex formation were obtained from cotton rats (*Sigmodon hispidus*) more than 4 months after oral infection with 50 parasite eggs. To isolate protoscoleces, the mature larval parasites were minced with scissors, pushed through a metal mesh, and washed repeatedly with physiological saline until host materials were thoroughly removed.

Preparation of enriched mitochondrial fractions. The enriched mitochondrial fractions of *E. multilocularis* protoscoleces were prepared essentially according to methods described previously for isolating adult *Ascaris* mitochondria (25, 26). Briefly, the isolated protoscolex sediment was suspended in 5 volumes of mitochondrial preparation buffer (210 mM mannitol, 10 mM sucrose, 1 mM disodium EDTA, and 50 mM Tris-HCl [pH 7.5]) supplemented with 10 mM sodium malonate. The parasite materials were homogenized with a motor-driven glass/glass homogenizer (six passes three to four times). The homogenate was diluted with the mitochondrial preparation buffer to 10 times the volume of the original protoscolex sediment and then centrifuged at 800 × *g* for 10 min to precipitate cell debris and nuclei. The supernatant was then centrifuged at 8,000 × *g* for 10 min to obtain the mitochondrial pellet. The pellet was resuspended in mitochondrial preparation buffer (without malonate) and centrifuged at 12,000 × *g* for 10 min. The resulting enriched mitochondrial fraction was suspended in mitochondrial preparation buffer (without malonate). The protein concentration was determined according to the method of Lowry et al. by using bovine serum albumin as a standard (15).

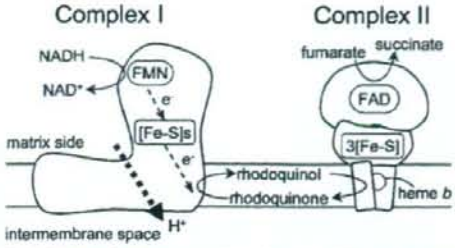

FIG. 2. Schematic representation of the NADH-fumarate reductase system in adult *A. suum*, which catalyzes the final step of the phosphoenolpyruvate carboxykinase-succinate pathway. In this system, the reducing equivalent of NADH is transferred to the low-potential RQ by the NADH-RQ reductase activity of mitochondrial complex I. This pathway ends with the production of succinate by the rhodoquinol-fumarate reductase activity of complex II. Electron transfer from NADH to fumarate is coupled to the site I phosphorylation of complex I via the generation of a proton-motive force. FMN, flavin mononucleotide; FAD, flavin adenine dinucleotide; [Fe-S]s and 3[Fe-S], iron-sulfur clusters.

Western blotting. An enriched mitochondrial fraction prepared from *E. multilocularis* protoscoleces and that from the liver of a cotton rat (used as the host animal for the parasite) were analyzed by Western blotting. Reactions were performed according to a method described previously by Towbin et al. (30). The proteins were separated by sodium dodecyl sulfate-polyacrylamide gel electrophoresis on a 10% or 15% acrylamide gel and electrophoretically transferred onto a nitrocellulose membrane. The membrane was soaked in 1:5,000 anti-cytochrome *c* oxidase subunit IV antibody (component of the ApoAlert cell fractionation kit; Clontech Laboratories) in phosphate-buffered saline containing 0.05% (wt/vol) Tween 20 and 2% (wt/vol) skim milk. The membrane was incubated for 60 min at room temperature and then washed three times for 10 min with washing buffer, which consisted of 0.05% (wt/vol) Tween 20 in phosphate-buffered saline. Alkaline phosphatase-conjugated goat anti-mouse immunoglobulin G was then added as a secondary antibody, and the mixture was incubated for 30 min. After another wash with washing buffer, the membrane was soaked in reaction buffer (100 mM Tris-HCl [pH 9.5], 100 mM NaCl, 5 mM $MgCl_2$, 500 μg/ml of 4-nitroblue tetrazolium chloride, and 165 μg/ml of 5-bromo-4-chloro-3-indolylphosphate) to initiate the development of a colored product. Finally, the membrane was washed with distilled water to stop the reaction. For Western blotting, the amounts of parasite and cotton rat mitochondrial samples were normalized by the total protein amount or cytochrome *c* oxidase activity (see below).

Enzyme assays. All enzyme assays using the enriched mitochondrial fractions were performed in a 0.7- or 1-ml reaction mixture at 25°C. The reagents used in each assay were mixed with reaction buffer containing 30 mM potassium phosphate (pH 7.4) and 1 mM $MgCl_2$. The final mitochondrial protein concentration was 80 μg per ml of reaction mixture. For all reactions performed under anaerobic conditions, the reaction medium was supplemented with 100 μg/ml glucose oxidase, 2 μg/ml catalase, and 10 mM β-D-glucose and left for 3 min to achieve anaerobiosis. NADH oxidase activity in the isolated mitochondrial fraction was determined in the presence or absence of 2 mM KCN, 100 mM malonate, or both by measuring the absorbance of NADH at 340 nm ($\varepsilon = 6.2\ mM^{-1}\ cm^{-1}$). The reaction was initiated by the addition of 100 μM of NADH to the mixture. Succinate dehydrogenase (SDH) activity was determined by monitoring the absorbance change of 2-(4,5-dimethyl-2-thiazolyl)-3,5-diphenyl-2*H*-tetrazolium bromide (MTT; 60 μg/ml) at 570 nm in the presence of 120 μg/ml phenazine methosulfate and 2 mM KCN. The reaction was initiated by the addition 10 mM of succinate to the mixture. Succinate-quinone reductase activity was assayed under aerobic or anaerobic conditions in the presence of 0.1%(wt/vol) sucrose monolaurate by determining the amount of decyl UQ (dUQ) or decyl RQ (dRQ)

from the absorbance change at 278 nm (ε = 12.7 mM^{-1} cm^{-1}) or 287 nm (ε = 9.2 mM^{-1} cm^{-1}), respectively. Decyl rhodoquinol-fumarate reductase activity was measured under anaerobic conditions in a reaction mixture containing 0.1% (wt/vol) sucrose monolaurate. In this reaction, 60 μM dRQ was reduced to decyl rhodoquinol in the cuvette by adding 200 μM $NaBH_4$. The reaction was started by adding 5 mM fumarate to the mixture, and the oxidation of decyl rhodoquinol was monitored at 287 nm. NADH-fumarate reductase activity was determined by monitoring the oxidation of NADH (100 μM) at 340 nm under anaerobic conditions. The reaction was initiated by the addition of 5 mM fumarate as an electron acceptor. NADH-quinone reductase activity assays were carried out under anaerobic conditions using the same reaction mixture as that used for the NADH-fumarate reductase activity assay except that 60 μM dUQ or dRQ was used as an electron acceptor instead of fumarate. The enzyme activity was determined by monitoring the absorbance change of NADH at 340 nm. Ubiquinol oxidase activity was determined by monitoring the absorbance change of ubiquinol-1 (150 μM) at 278 nm (ε = 12.7 mM^{-1} cm^{-1}) in the presence or absence of 2 mM KCN. The activity of cytochrome *c* oxidase was determined as *N,N,N′,N′*-tetramethyl-*p*-phenylenediamine dihydrochloride (TMPD) oxidase activity, which was measured by monitoring the absorbance change of TMPD (500 μM) at 610 nm (ε = 11.0 mM^{-1} cm^{-1}) in the presence or absence of 2 mM KCN.

Enzyme inhibition assays. Based on the findings of Yamashita et al. showing that that quinazoline-type compounds inhibit the NADH-quinone reductase activity of *A. suum* complex I (35), we determined 50% inhibitory concentration (IC_{50}) values of the quionazoline-type compounds against NADH-fumarate reductase activity of the parasite mitochondria and the NADH oxidase activity of bovine heart mitochondria (see "Enzyme assays"). The compounds used in the assays included quinazoline and its derivatives 6-NH_2, 6-NHCO($CH{=}CH_2$), 7-NH_2, 8-OH, 8-OCH_3, 8-OCH_2CH_3, and 8-$OCH(CH_3)_2$.

Analysis of the quinone profile of isolated mitochondria. Quinones were extracted from lyophilized mitochondria essentially according to a method described previously by Takada et al. (24). A lyophilized mitochondrial sample (2.9 mg protein) was crushed into powder before extraction, vortexed in 2:5 (vol/vol) ethanol/*n*-hexane for 10 min, and centrifuged at 20,000 × *g* for 5 min at room temperature. The supernatants were pooled, and the extraction of quinones was repeated twice. Pooled extracts were evaporated to dryness, dissolved in ethanol, and kept in the dark until high-performance liquid chromatography (HPLC) analysis. Quinones were applied to a reverse-phase HPLC column (Inertsil ODS-3 [5 μm and 4.6 by 250 mm]; GL Science) and eluted under isocratic conditions (1 ml/min) with 1:4 (vol/vol) diisopropyl ether-methanol at 25°C. The molecular species of the eluted quinones were identified by their retention times and by their spectral characteristics as measured with a UV-visible photodiode array (Shimadzu SPD-10-A). The concentration of quinones was determined spectrophotometrically. The major quinone detected was confirmed by mass spectrometry (MS) using an Applied Biosystems API-165 LC/MS system with electrospray ionization.

In vitro treatment of *E. multilocularis* protoscoleces. *E. multilocularis* protoscoleces were obtained as described above (see "Isolation of *E. multilocularis* protoscoleces"). The parasite materials were placed into culture medium suitable for the long-term maintenance of the protoscoleces in vitro (27). The parasite cultures were kept in a six-well plate at a density of approximately 500 protoscoleces per ml of culture medium, and half of the medium was replaced twice a week. This culture condition was also applied during in vitro treatment of the parasite. To examine the efficacy of chemical compounds against living *E. multilocularis* protoscoleces, the parasites were kept in the culture medium supplemented with 5 or 50 μM of each compound, including quinazoline and its 8-OH derivative, rotenone (a specific inhibitor of mitochondrial complex I) (19) and nitazoxanide (a compound with strong protoscolicidal action) (32). One control group was supplemented with 0.5% (vol/vol) dimethyl sulfoxide (vehicle) alone, and all conditions were assayed in triplicate. The viability of protoscoleces was determined by microscopic analysis of more than 170 protoscoleces per well for motile behavior and the ability to exclude trypan blue (32).

RESULTS

Preparation of enriched mitochondrial fractions. To characterize the mitochondrial respiratory chain of *E. multilocularis* protoscoleces, we prepared enriched mitochondrial fractions from the parasite. Approximately 80 g of larval *E. multilocularis* (containing approximately 10^5 protoscoleces per gram) was obtained from each cotton rat more than 4 months after oral infection with 50 parasite eggs. Approximately 20 g of the larval parasite was used per isolation of protoscoleces, yielding 2 ml of cleaned protoscolex sediment (Fig. 3). The enriched mitochondrial fractions were prepared from the protoscolex sediment as described in Materials and Methods. Each 1 ml of protoscolex sediment (containing 4.5 × 10^5 protoscoleces) yielded approximately 4 mg of mitochondria. Western blotting using an antibody to mammalian cytochrome *c* oxidase detected a specific band in the mitochondria from the liver of a cotton rat but not in mitochondria from *E. multilocularis* protoscoleces even when the amounts of both mitochondrial samples were normalized according to cytochrome *c* oxidase activity (data not shown). These results demonstrated that the enriched mitochondrial fractions from the parasite were sufficiently free of host components for use in enzyme assays and quinone analyses. In order to assess the quality of mitochondria, intactness was examined by the reactivity of NADH, which is a non-membrane-permeable substrate. NADH oxidase activity was not detected in the isotonic buffer, whereas it was fully activated in hypotonic buffer after a freeze-thaw treatment of the enriched mitochondrial fraction. Based on the results obtained, the method applied here for mitochondrial preparation seemed to be appropriate.

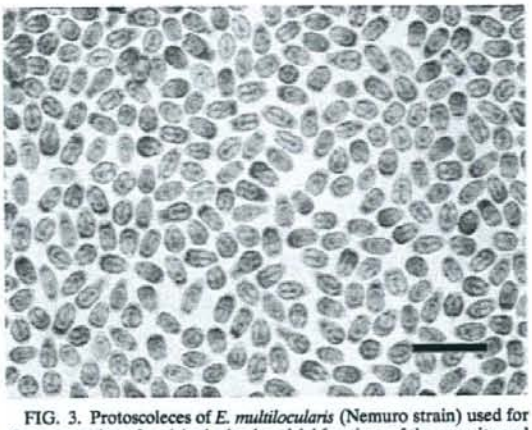

FIG. 3. Protoscoleces of *E. multilocularis* (Nemuro strain) used for the preparation of enriched mitochondrial fractions of the parasite and subsequent analyses. Bar, 500 μm.

Enzyme activities of *E. multilocularis* mitochondria. The specific enzyme activities involved in the mitochondrial respiratory chain of *E. multilocularis* protoscoleces are shown in Table 1. Parasite complex II exhibited an SDH activity of 103 nmol/min/mg. The specific activity of succinate-dUQ reductase was comparable to that of SDH activity (98.9 nmol/min/mg), whereas the succinate-dRQ reductase activity was lower (16.6 nmol/min/mg). The specific activity of decyl rhodoquinol-fumarate reductase, which is the reverse reaction of the succinate-RQ reductase activity of complex II, was determined to be 60.2 nmol/min/mg. The mitochondria of *E. multilocularis* protoscoleces exhibited NADH oxidase activity of 9.1 nmol/min/mg, which was almost eliminated by 2 mM KCN and 100 mM malonate. Ubiquinol-1 oxidase and TMPD oxidase activities were determined to be 4.4 nmol/min/mg and 12.6 nmol/